7-2-2020

Tri- and Tetrameric Proanthocyanidins with Dentin Bioactivities from *Pinus massoniana*

Bin Zhou
University of Illinois at Chicago

Yvette Alania
Marquette University

Mariana C. Reis
University of Illinois at Chicago

Rasika S. Phansalkar
University of Illinois at Chicago

Joo-Won Nam
University of Illinois at Chicago

See next page for additional authors

Journal of Organic Chemistry, Vol. 85, No. 13 (July 2, 2020): 8462-8479. DOI.

Tri- and Tetrameric Proanthocyanidins with Dentin Bioactivities from *Pinus massoniana*

Bin Zhou
Department of Pharmaceutical Sciences, College of Pharmacy, University of Illinois at Chicago, Chicago, Illinois
Yvette Alania
Department of Restorative Dentistry, College of Dentistry, University of Illinois at Chicago, Chicago, Illinois
Mariana Reis
Department of Restorative Dentistry, College of Dentistry, University of Illinois at Chicago, Chicago, Illinois
Rasika S. Phansalkar
Department of Pharmaceutical Sciences, College of Pharmacy, University of Illinois at Chicago, Chicago, Illinois
Joo-Won Nam
Department of Pharmaceutical Sciences, College of Pharmacy, University of Illinois at Chicago, Chicago, Illinois
College of Pharmacy, Yeungnam University, Gyeongsan, Gyeongbuk 712-749, Korea

James B. McAlpine
Department of Pharmaceutical Sciences, College of Pharmacy, University of Illinois at Chicago, Chicago, Illinois
Program for Collaborative Research in the Pharmaceutical Sciences (PCPRS), College of Pharmacy, University of Illinois at Chicago, Chicago, Illinois
Shao-Nong Chen
Department of Pharmaceutical Sciences, College of Pharmacy, University of Illinois at Chicago, Chicago, Illinois
Program for Collaborative Research in the Pharmaceutical Sciences (PCPRS), College of Pharmacy, University of Illinois at Chicago, Chicago, Illinois
Ana K. Bedran-Russo
Department of Restorative Dentistry, College of Dentistry, University of Illinois at Chicago, Chicago, Illinois
Guido F. Pauli
Department of Pharmaceutical Sciences, College of Pharmacy, University of Illinois at Chicago, Chicago, Illinois
Program for Collaborative Research in the Pharmaceutical Sciences (PCPRS), College of Pharmacy, University of Illinois at Chicago, Chicago, Illinois

Abstract

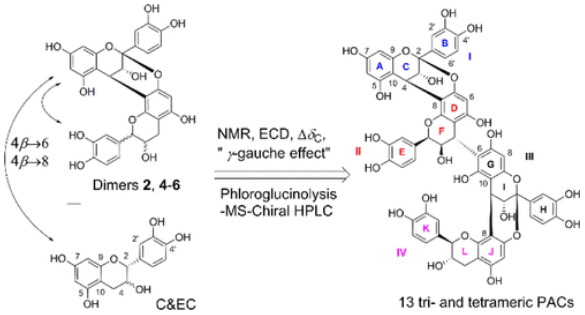

Guided by dentin biomechanical bioactivity, this phytochemical study led to the elucidation of an extended set of structurally demanding proanthocyanidins (PACs). Unambiguous structure determination involved detailed spectroscopic and chemical characterization of four A-type dimers (**2** and **4–6**), seven trimers (**10–16**), and six tetramers (**17–22**). New outcomes confirm the feasibility of determining the absolute configuration of the catechol monomers in oligomeric PACs by one-dimensional (1D) and two-dimensional (2D) NMR. Electronic circular dichroism as well as phloroglucinolysis followed by mass spectrometry and chiral phase high-performance liquid chromatography (HPLC) analysis generated the necessary chiral reference data. In the context of previously reported dentin-bioactive PACs, accurately and precisely assigned ^{13}C NMR resonances enabled absolute stereochemical assignments of PAC monomers via (i) inclusion of the ^{13}C NMR γ-gauche effect and (ii) determination of differential ^{13}C chemical shift values ($\Delta\delta_C$) in comparison with those of the terminal monomer (unit II) in the dimers **2** and **4–6**. Among the 13 fully elucidated PACs,

eight were identified as new, and one structure (**11**) was revised based on new knowledge gained regarding the subtle, stereospecific spectroscopic properties of PACs.

Introduction

Proanthocyanidins (PACs) are a structurally diverse and complex group of condensed, oligomeric flavan-3-ols that are widespread in woody and some herbaceous plants.(1) PACs contain several subtypes such as procyanidins, prodelphinidins, and propelargonidins based on the corresponding basic units catechin and epi-catechin (syn. epicatechin), gallocatechin and epi-gallocatechin (syn. epigallocatechin), and afzelechin and epi-afzelechin (syn. epiafzelechin).(2) B-type PACs have one interflavanyl bond originated from coupling C-4 with one of the nucleophilic C-6 or C-8 of a subsequent monomer. A-type PACs have an additional ether bond between C-2 in the "top" and an A-ring hydroxyl moiety in the "bottom" unit. Since their discovery in 1947, PACs have attracted scientific attention for their complicated structures and medicinal values.(3) While PACs have been associated with a broad spectrum of bioactivities, including antioxidant,(4) anticancer,(5) anti-inflammatory,(6) antidiabetic,(7) neuroprotective(8) effects, and play an important role in the fields of nutrition and health. The focus of our research at the chemistry–dentistry interface has been the exploration and understanding of their structure-specific abilities to enhance the biomechanical properties of dentin, the collagenous tissue of teeth.(9−11)

The structural complexity of PACs increases exponentially with their degree of polymerization (DP), the linkages (A- and B-type), and absolute configuration of their interflavanyl linkages (IFLs), as well as the combination of the possible stereoisomeric monomers. Additional analytical challenges are posed by the formation of atropisomers, which interferes with chromatographic separation and often makes NMR spectra acquired at room temperature uninterpretable because of exceedingly broad lines. Additionally, in some cases, resonances can be "missing" because of H–D exchange in deuterated NMR solvents, even for hydrogens that might initially be considered "not likely to exchange."(9−11) Collectively, these properties make the structural elucidation of trimeric or higher oligomeric PACs an often challenging undertaking. In general, reliance on the literature data is hazardous as structure-related publications seldom report full assignment of the ^{1}H and ^{13}C NMR data. This provides grounds for questioning the ultimate reliability of at least some PAC structures and their spectroscopic assignments and rationalizes the importance of developing highly cohesive data sets.

Pinus massoniana is a pine species within the Pinaceae family that has a PAC-rich inner bark. Our previous studies showed that *P. massoniana* PACs can specifically enhance dentin biomechanical properties and reduce proteolytic dentin degradation.(9−11) Studies of PACs action on dentin initially established that the affinity of PACs for type-I collagen correlates with the DP and certain structural/stereochemical features.(9−11) These previous studies showed that tri- and tetrameric PACs are the most promising dentin strengthening agents. Accordingly, this study was focused on phytochemical isolation and structural analysis of tri- and tetrameric PACs from *P. massoniana* pine bark. Carried out in a scaled-up operation, the goal was to provide solid structural evidence for these PACs and sufficient amounts of the most bioactive PAC oligomers required to explore their mechanism of action on dentin, including a variety of biomechanical properties such as static and dynamic stiffness, biodegradation resistance, and resin bonding properties.

In addition to the four known A-type dimers, epicatechin-(2β → O → 7,4β → 8)-catechin (**2**),(9) epicatechin-(2β → O → 7,4β → 8)-epicatechin (**4**),(9) epicatechin-(2β → O → 7,4β → 8)-*ent*-catechin (**5**),(10) and epicatechin-(2β → O → 7,4β → 8)-*ent*-epicatechin (**6**)(10) reported previously from this plant, seven trimers (**10–16**) and six tetramers (**17–22**) were isolated and characterized (Figure 1). Among these 13 PACs, eight are new structures, and one (**11**)(9) was revised based on new NMR evidence. In order to achieve rigorous structural evidence for these PACs, the following strategies were applied: (i) all NMR data sets were acquired at low temperatures (278 and/or 255 K) to achieve assignable spectra with high resolution, (ii) two-dimensional (2D) heteronuclear single quantum coherence, heteronuclear multiple bond correlation (HMBC), and nuclear Overhauser enhancement spectroscopy (NOESY) spectra were used to establish the planar structures; particularly, 4 → 6 and 4 → 8 IFLs can be distinguished from the NOESY data, by the differential chemical shifts of the C-6 and C-8 atoms in the monomers. The absolute configuration of the constituent monomers were determined by a combination of (iii) NMR evidence involving NOESY correlations, the "γ-gauche effect" in the ^{13}C domain, differential ^{13}C chemical shift ($\Delta\delta_C$) values relative to the four stereochemically fully characterized dimers (terminal unit II), (iv) electronic circular dichroism (ECD) data, and (v) phloroglucinolysis combined with liquid chromatography–mass spectrometry (MS) and chiral phase high-performance liquid chromatography (HPLC) analysis (Figures 5 and S104–S106, Supporting Information). Factoring in previously reported NMR assignment, these spectroscopic and chemical methods allowed the unambiguous assignment of the structures of all isolated PACs. The presented detailed analytical profiles of 13 PACs (Tables 1–10, sorted by $^{1}H/^{13}C$ domains and increasing degree of oligomerization) enlarge significantly the space of the available NMR data of oligomeric PACs with solid structural information. This also expands the library of PACs that can be used to explore their dentin biomodification mechanisms of action systematically and supports the ongoing establishment of structure–activity relationships.

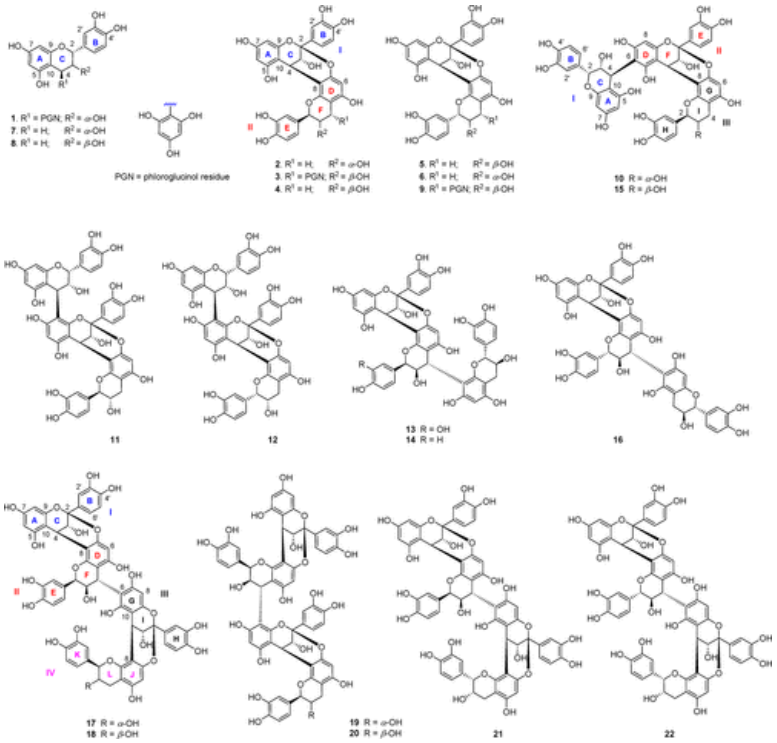

Figure 1. Structures of **1–22**. Compounds **1**, **3**, and **9** represent the phloroglucinol (PGN) adducts.

Table 1. ^{1}H and ^{13}C NMR (400/100 MHz, resp.) Data of 1, 3, and 9 in CD_3OD

			1a		3b		9b	
unit	**ring**	**no.**	**δ_H mult (*J* in Hz)**	**^{13}C**	**δ_H mult (*J* in Hz)**	**^{13}C**	**δ_H mult (*J* in Hz)**	**^{13}C**
I	C	2	5.03, brs	77.1		100.1		100.3
		3	3.89, dd (2.0, 1.0)	73.2	4.05, d, (3.4)	68.3	4.13, d, (3.5)	67.8
		4	4.49, dd (2.0, 0.9)	37.0	4.45, d, (3.4)	29.5	4.20, d, (3.5)	29.5
	A	5		157.6c		157.1		156.8
		6	AB	AB	6.03, d (2.4)	98.3	5.89, d (2.4)	98.0
		7		157.8c		158.1		158.2
		8	AB	AB	6.08, d (2.4)	96.7	6.04, d (2.4)	96.5
		9		158.1c		154.2		154.0
		10		101.7		104.4		103.9
	B	1′		132.7		132.6		132.4
		2′	6.87, d (1.9)	115.0	7.16, d (2.1)	115.7	7.13, d (2.2)	115.7
		3′		145.8		145.6		145.6
		4′		145.5		146.7		146.8
		5′	6.71, d (8.2)	115.7	6.82, d (8.4)	115.6	6.80, d (8.4)	115.6
		6′	6.71, dd (8.2, 1.9)	119.1	7.03, dd (8.4, 2.1)	119.8	7.01, dd (8.4, 2.2)	119.9
II	F	2			5.31, brs	79.1	4.54, d (9.8)	84.5
		3			3.98, brd (1.9)	72.9	4.57, dd (9.8, 8.4)	73.0
		4			4.56, brs	37.9	4.48, brd (8.4)	38.6
	D	5				157.0		156.1
		6			6.06, s	96.3	5.97, s	97.6
		7				152.4		151.9
		8				106.8		107.0
		9				152.4		152.2
		10				105.6		108.8
	E	1′				131.8		131.3
		2′			7.13, d (2.1)	116.2	7.07, d (2.1)	116.3
		3′				145.9		146.2
		4′				146.2		146.8
		5′			6.80, d (8.3)	116.1	6.84, d (8.2)	116.2
		6′			6.96, dd (8.3, 2.1)	120.6	6.95, dd (8.2, 2.1)	121.1
phloroglucinol		1″		107.4		AB		107.5
		2″ & 6″		158.7		AB		159.7
		3″ & 5″	5.75, s	95.1	AB	AB	5.79, s	95.5

		4″		160.0		AB		160.1

[a]NMR data were acquired at 255 K.

[b]NMR data were acquired at 298 K.

[c]Interchangeable assignment; AB: absence of signals.

Table 2. ^{13}C NMR Data (CD_3OD, 100 MHz) of Dimers 2 and 4–6 Acquired at Three Different Temperatures: 255, 278, and 298 K

			2			**4**			**5**			**6**		
			δ_C			**δ_C**			**δ_C**			**δ_C**		
unit	**ring**	**no.**	**298 K**	**278 K**	**255 K**	**298 K**	**278 K**	**255 K**	**298 K**	**278 K**	**255 K**	**298 K**	**278 K**	**255 K**
I	C	2	100.28	100.22	100.13	100.16	100.05	99.94	100.40	100.32	100.24	100.42	100.37	100.30
		3	67.74	67.75	67.71	68.06	67.99	67.98	67.64	67.56	67.50	67.73	67.70	67.65
		4	29.16	29.13	29.12	29.23	29.13	29.05	29.22	29.12	29.03	29.23	29.17	29.07
	A	5	156.71	156.78	156.84	156.99	156.98	157.00	156.66	156.63	156.64	156.70	156.73	156.72
		6	98.14	98.01	97.83	98.29	98.11	97.92	98.14	98.02	97.89	97.95	97.84	97.71
		7	158.08	158.11	158.06	158.11	158.03	158.00	158.12	158.10	158.05	158.10	158.10	158.05
		8	96.52	96.39	96.26	96.61	96.49	96.36	96.58	96.47	96.35	96.54	96.43	96.31
		9	154.19	154.19	154.16	154.24	154.18	154.14	154.08	154.02	153.98	154.14	154.12	154.06
		10	104.00	103.89	103.76	104.25	104.12	103.98	104.03	103.91	103.80	104.06	103.97	103.86
	B	1′	132.24	132.22	132.15	132.43	132.34	132.28	132.21	132.10	132.01	132.30	132.24	132.16
		2′	115.66	115.59	115.48	115.65	115.54	115.43	115.71	115.60	115.50	115.63	115.53	115.43
		3′	145.59	145.61	146.70	145.64	145.57	145.52	145.65	145.59	145.55	145.65	145.64	145.60
		4′	146.73	146.74	145.56	146.75	146.67	146.62	146.80	146.74	146.69	146.78	146.76	146.72
		5′	115.62	115.51	115.41	115.54	115.53	115.43	115.63	115.54	115.43	115.70	115.67	115.52
		6′	119.81	119.77	119.71	119.78	119.72	119.67	119.85	119.79	119.74	119.85	119.8	119.75
II	F	2	84.41	84.43	84.36	81.73	81.60	81.48	83.87	83.80	83.75	80.82	80.74	80.61
		3	68.06	68.09	68.10	66.96	66.93	66.97	68.38	68.32	68.29	67.13	67.10	67.05
		4	28.90	29.04	29.04	29.88	29.87	29.90	28.83	28.84	28.90	29.46	29.51	29.55
	D	5	156.09	156.15	156.14	156.59	156.55	156.56	156.15	156.14	156.16	156.62	156.65	156.66
		6	96.52	96.39	96.20	96.48	96.31	96.12	96.52	96.37	96.22	96.46	96.30	96.14
		7	152.14	152.19	152.20	152.28	152.24	152.24	152.21	152.17	152.16	152.06	152.05	152.02
		8	106.75	106.69	106.60	107.20	107.10	107.03	106.54	106.40	106.29	106.92	106.84	106.75
		9	151.36	151.41	151.42	152.13	152.13	152.18	150.83	150.80	150.79	151.28	151.28	151.27
		10	103.09	103.01	102.89	102.41	102.28	102.21	102.81	102.69	102.58	101.89	101.78	101.66
	E	1′	130.51	130.47	130.39	131.19	131.18	131.22	130.92	130.77	130.63	131.40	131.37	131.33

		2′	115.71	115.65	115.56	115.92	115.79	115.64	115.42	115.30	115.18	115.20	115.07	114.91
		3′	146.29	146.30	146.25	145.97	145.88	145.81	146.41	146.35	146.33	146.20	146.2	146.16
		4′	146.73	146.74	146.70	146.28	146.17	146.08	146.75	146.70	146.69	146.20	146.17	146.11
		5′	116.31	116.22	116.10	116.03	115.92	115.81	116.34	116.24	116.14	116.19	116.09	115.98
		6′	120.68	120.66	120.64	120.37	120.29	120.18	120.33	120.30	120.31	119.42	119.30	119.15

Table 3. ^{1}H NMR Data of 10–14 (CD_3OD, 800 MHz)

			10a		**11b**	**12b**	**13b**	**14b**	
			δ_H mult (*J* in Hz)		**δ_H mult (*J* in Hz)**	**δ_H mult (*J* in Hz)**	**δ_H mult (*J* in Hz)**	**δ_H mult (*J* in Hz)**	
unit	**ring**	**no.**	**rotamer A**	**rotamer B**	**major**	**major**	**major**	**major A**	**minor B**
I	C	2	5.48, s	5.05, s	5.10, s	5.01, s			
		3	3.80, brs	3.88, brs	3.96, brs	3.89, brs	3.45, d (3.5)	3.46, d (3.5)	4.07, d (3.3)
		4	4.64, brs	4.65, brs	4.82, brd (1.9)	4.77, brs	3.99, d (3.5)	3.99, d (3.5)	4.42, d (3.3)
	A	6	5.86, d (1.7)	5.92, d (1.7)	6.00, brs	5.95, d (1.9)	5.92, d (2.4)	5.92, d (2.3)	6.01, d (2.3)
		8	6.17, d (1.7)	5.98, d (1.7)	6.04, brs	5.98, d (1.9)	5.99, d (2.4)	5.99, d (2.3)	6.06, d (2.3)
	B	2′	6.93, d (2.1)	6.85, d (2.1)	6.87, d (1.8)	6.80, d (2.0)	7.08, d (2.2)	7.08, d (2.2)	7.14, d (2.2)
		5′	6.72, d (8.2)	6.68, d (8.2)	6.72, d (8.3)	6.66, d (8.2)	6.85, d (8.2)	6.85, d (8.2)	6.81, d (8.3)
		6′	6.61, dd (8.2, 2.1)	6.64, dd (8.2, 2.1)	6.68, dd (8.3, 1.8)	6.61, dd (8.2, 2.0)	6.93, dd (8.2, 2.2)	6.93, dd (8.2, 2.2)	7.02, dd (8.3, 2.2)
II	F	2					5.51, s	5.56, s	5.39, s
		3	4.05, d (3.6)	4.09, d (3.5)	4.18, d (3.5)	4.23, d (3.4)	4.04, brd (1.9)	4.06, brd (1.9)	4.00, brs
		4	4.06, d (3.6)	4.19, d (3.5)	4.35, d (3.5)	4.49, d (3.4)	4.53, brs	4.54, brs	4.72, brs
	D	6			5.98, s	5.85, s	5.82, s	5.83, s	6.08, s
		8	6.20, s	6.03, s					
	E	2′	7.09, d (2.2)	7.11, d (2.2)	7.35, d (2.0)	7.30, d (2.2)	7.23, d (2.1)	7.61, brd (8.7)	7.48, brd (8.6)
		3′						6.86, brd (8.7)	6.81, brd (8.6)
		5′	6.81, d (8.1)	6.79, d (8.1)	6.85, d (8.1)	6.81, d (8.2)	6.84, d (8.2)	6.86, brd (8.7)	6.81, brd (8.6)
		6′	7.00, dd (8.1, 2.2)	7.01, dd (8.1, 2.2)	7.22, dd (8.1, 2.0)	7.19, dd (8.2, 2.2)	7.09, dd (8.2, 2.1)	7.61, brd (8.7)	7.48, brd (8.6)
III	I	2	4.36, d (9.4)	4.75, d (8.2)	4.78, d (7.9)	5.06, s	3.94, d (9.2)	3.96, d (9.1)	4.94, d (5.5)
		3	4.20, ddd (10.0, 9.4, 6.2)	3.89, ddd (8.8, 8.2, 5.6)	4.20, ddd (8.4, 7.9, 5.0)	4.26, dd (4.3, 2.0)	3.66, ddd (10.3, 9.2, 6.2)	3.66, ddd (10.2, 9.1, 6.2)	4.13, m
		4	2.47, dd (−16.2, 10.0)	2.57, dd (−16.2, 8.8)	3.02, dd (−16.2, 5.0)	2.87, dd (−16.9, 2.0)	2.41, dd (−16.1, 10.3)	2.41, dd (−16.1, 10.2)	2.63, m

			3.08, dd (−16.2, 6.2)	3.00, dd (−16.2, 5.6)	2.62, dd (−16.2, 8.4)	2.94, dd (−16.9, 4.3)	3.04, dd (−16.1, 6.2)	3.04, dd (−16.1, 6.2)	2.63, m
	G	6	6.11, s	6.11, s	6.09, s	6.03, s	6.09, s	6.10, s	5.86, s
	H	2′	6.74, d (2.2)	6.99, d (2.2)	6.98, d (1.6)	7.15, d (2.1)	6.75, d (2.0)	6.77, d (2.1)	6.87, d (2.2)
		5′	7.03, d (8.1)	6.86, d (8.1)	6.84, d (8.4)	6.84, d (8.2)	6.76, d (8.1)	6.73, d (8.1)	6.71, d (8.2)
		6′	6.79, dd (8.1, 2.2)	6.91, dd (8.1, 2.2)	6.88, dd (8.4, 1.6)	6.95, dd (8.2, 2.1)	6.67, dd (8.1, 2.0)	6.65, dd (8.1, 2.1)	6.88, dd (8.2, 2.2)

[a]NMR data were acquired at 255 K.

[b]NMR data were acquired at 278 K.

Table 4. ^{1}H NMR Data of 15, 16, and 22 (CD_3OD, 800 MHz)

			15b		**16c**		**22c**
			δ_H mult (*J* in Hz)		**δ_H mult (*J* in Hz)**		**δ_H mult (*J* in Hz)**
unit	**ring**	**no.**	**major A**	**minor B**	**rotamer A**	**rotamer B**	**major**
I	C	2	5.04, s	5.63, s			
		3	3.92, d (1.8)	3.96, d (1.8)	4.12, d (3.4)	4.09, d (3.4)	4.25, d (3.5)
		4	4.65, d (1.8)	4.66, d (1.8)	4.21, d (3.4)	4.19, d (3.4)	3.91, d (3.5)
	A	6	5.92, d (1.7)	5.86, brs	5.89, d (2.4)	5.89, d (2.4)	5.84, d (2.4)
		8	5.98, d (1.7)	6.17, brs	6.04, d (2.4)	6.04, d (2.4)	6.03, d (2.4)
	B	2′	6.86, d (2.1)	7.00, d (2.1)	7.10, d (2.2)	7.11, d (2.2)	7.16, d (2.1)
		5′	6.70, d (8.1)	6.72, d (8.2)	6.79, d (8.3)	6.79, d (8.3)	6.80, d (8.2)
		6′	6.64, dd (8.1, 2.1)	6.88, dd (8.2, 2.1)	6.98, dd (8.3, 2.2)	6.99, dd (8.3, 2.2)	7.03, dd (8.2, 2.1)
II	F	2			4.57a	4.54a	4.34, d (9.8)
		3	4.14, d (3.5)	4.00, d (3.6)	4.53a	4.51a	4.37, dd (9.8, 7.8)
		4	4.33, d (3.5)	4.19, d (3.6)	4.55a	4.43, d (7.6)	4.44, d (7.8)
	D	6			6.00, s	5.98, s	5.86, s
		8	6.04, s	6.21, s			
	E	2′	7.13, d (2.2)	7.10, d (2.2)	7.07, d (2.2)	7.07, d (2.2)	6.99, d (2.2)
		5′	6.82, d (8.1)	6.79, d (8.1)	6.84, d (8.2)	6.84, d (8.2)	6.89, d (8.1)
		6′	7.03, dd (8.1, 2.2)	6.99, dd (8.1, 2.2)	6.96, dd (8.2, 2.2)	6.96, dd (8.2, 2.2)	6.80, dd (8.1, 2.2)
III	I	2	4.95, s	4.76, s	4.50a	4.57a	
		3	4.17, m	3.98, m	3.97a	3.98a	4.14, d (3.6)
		4	2.83, brd (−16.9)	2.79, brd (−16.5)	2.46, dd (−15.8, 8.4)	2.60, dd (−16.1, 8.2)	4.34, d (3.6)

			3.00, dd (−16.9, 4.5)	2.90, dd (−16.5, 4.2)	2.78, dd (−15.8, 5.4)	2.91, dd (−16.1, 5.3)	
	G	6	6.13, s	6.12, s			
		8			6.00, s	5.90, s	6.18, s
	H	2′	7.29, d (2.2)	6.84, d (2.2)	6.84, d (2.0)	6.82, d (2.0)	7.13, d (2.2)
		5′	6.82, d (8.1)	6.97, d (8.1)	6.74, d (8.1)	6.75, d (8.1)	6.81, d (8.3)
		6′	6.99, dd (8.1, 2.2)	7.02, dd (8.1, 2.2)	6.72, dd (8.1, 2.0)	6.71, dd (8.1, 2.0)	7.02, dd (8.3, 2.2)
IV	L	2					5.21, brs
		3					4.32, m
		4					2.86, brd (−17.0)
							2.96, dd (−17.0, 4.4)
	J	6					6.07, s
	K	2′					7.28, d (2.1)
		5′					6.94, d (8.1)
		6′					7.12, dd (8.1, 2.1)

[a]Signals are overlapped.

[b]NMR data were acquired at 255 K.

[c]NMR data were acquired at 278 K.

Table 5. ^{13}C NMR Data of 10–16 (CD_3OD, 100 MHz)

			10a		**11b**	**12b**	**13b**	**14b**		**15a**		**16b**	
			δ_C		**δ_C**	**δ_C**	**δ_C**	**δ_C**		**δ_C**		**δ_C**	
unit	**ring**	**no.**	**rotamer A**	**rotamer B**	**major**	**major**	**major**	**major A**	**minor B**	**major A**	**minor B**	**rotamer A**	**rotamer B**
I	C	2	77.7	77.0	77.1	77.1	100.0	100.0	100.0	76.7	78.0	100.2	100.2
		3	73.5	72.8	73.2	73.3	67.1	67.2	68.4	72.9	73.0	67.7	67.7
		4	36.7	37.5	37.1	37.2	28.8	28.8	29.4	37.5	36.6	29.4	29.4
	A	5	158.2	156.8	158.1	158.1	156.7	156.7	157.2	157.7	157.8	156.7	156.7
		6	95.6	95.5	95.9	96.3	98.3	98.2	98.2	95.6	95.9	97.8	97.8
		7	157.8	157.9	158.0	158.1	157.8	157.8	158.1	157.7	157.5	158.1	158.1
		8	95.3	95.7	96.3	96.1	96.4	96.4	96.5	95.6	95.3	96.4	96.4
		9	157.7	157.8	157.9	157.9	154.2	154.2	154.2	157.8	156.9	153.9	153.9
		10	103.4	102.2	101.9	101.9	105.0	104.9	104.2	102.1	103.2	103.7	103.8
	B	1′	132.9	132.6	132.5	132.6	132.4	132.4	132.6	132.0	132.7	132.2	132.2

		2′	115.2	115.1	115.1	115.1	115.7	115.8	115.6	115.0	115.5	115.5	115.5
		3′	145.9	145.8	145.7	145.8	145.5	145.5	145.6	145.5	145.5	145.5	145.5
		4′	145.6	145.5	145.4	145.5	146.6	146.6	146.7	145.8	145.5	146.7	146.7
		5′	115.8	115.6	115.8	115.8	115.7	115.6	115.8	115.6	115.8	115.5	115.5
		6′	119.4	119.1	119.3	119.3	120.0	120.0	119.7	119.1	120.1	119.8	119.8
II	F	2	99.9	100.1	100.5	100.8	78.6	78.5	79.0	100.0	99.7	84.8	84.8
		3	67.6	67.7	67.4	67.5	72.4	72.3	72.7	67.6	68.0	73.7	73.7
		4	29.1	29.6	29.3	29.5	38.3	38.2	37.7	29.5	29.0	38.7	39.5
	D	5	154.9	154.1	155.2	155.3	155.9	155.9	157.0	154.5	155.1	156.1	156.0
		6	111.3	110.6	99.2	99.0	95.9	95.9	96.1	110.4	110.9	97.6	97.3
		7	156.2	157.1	157.0	157.1	151.0	151.0	152.4	157.2	156.5	151.8	152.1
		8	96.4	97.5	108.3	108.4	106.1	106.1	106.6	97.4	96.5	107.0	106.8
		9	152.0	152.1	151.1	151.2	151.7	151.8	152.4	152.1	152.2	152.5	152.5
		10	104.2	103.9	103.8	103.9	106.5	106.4	105.8	104.2	103.8	108.5	108.8
	E	1′	132.1	132.1	132.2	132.3	131.5	130.8	130.3	132.5	132.1	131.1	131.1
		2′	115.5	115.5	115.5	115.6	116.5	130.6	131.2	115.5	115.5	116.0	116.0
		3′	145.6	145.6	145.6	145.7	146.0	116.0	115.8	145.6	145.4	146.1	146.1
		4′	146.7	146.8	146.7	146.8	146.3	158.3	158.2	146.7	146.6	146.7	146.7
		5′	115.4	115.4	115.7	115.7	116.1	116.0	115.8	115.4	115.5	116.0	116.0
		6′	119.7	119.7	120.0	120.1	121.0	130.6	131.2	119.8	119.7	121.0	121.0
III	I	2	85.7	85.2	84.4	80.8	83.2	83.2	81.9	82.8	82.6	82.5	82.5
		3	68.2	68.9	68.1	67.2	70.1	70.0	68.3	67.0	66.9	68.7	68.8
		4	31.2	29.2	29.2	29.6	30.7	30.7	26.6	30.7	30.4	28.7	29.2
	G	5	156.3	156.3	156.1	156.7	155.4	155.4	155.4	157.0	156.8	154.6	155.6
		6	96.7	96.4	96.3	96.3	96.3	96.3	96.9	96.6	96.5	110.7	110.9
		7	152.2	152.2	152.1	152.1	155.6	155.6	156.3	152.3	151.7	156.4	155.6
		8	106.9	106.3	106.8	107.0	108.7	108.7	108.2	106.8	106.5	96.0	97.1
		9	151.8	151.2	151.4	151.3	155.3	155.3	153.9	152.2	152.6	154.7	154.6
		10	103.8	103.1	103.1	101.9	101.5	101.5	100.3	101.9	102.4	101.9	101.5
	H	1′	129.6	129.9	130.4	131.4	132.6	132.7	132.5	130.4	131.0	132.0	132.0
		2′	117.9	115.8	115.8	115.1	115.7	115.6	114.3	116.3	115.8	115.1	115.1
		3′	145.1	146.2	146.2	146.2	145.8	146.0	146.1	145.8	145.5	146.1	146.1
		4′	146.5	146.9	146.7	146.2	145.8	145.8	145.8	146.7	146.2	146.1	146.1

		5′	118.2	116.6	116.3	116.1	116.1	116.0	116.0	115.9	117.2	116.0	116.0
		6′	119.6	121.2	120.8	119.3	119.9	120.0	119.3	121.3	120.9	120.0	120.0

[a]NMR data were acquired at 255 K.

[b]NMR data were acquired at 278 K.

Table 6. ^{1}H NMR Data of 17–21 (CD_3OD, 800 MHz, 278 K)

			17	18	19		20		21	
			δ_H mult (*J* in Hz)	**δ_H mult (*J* in Hz)**	**δ_H mult (*J* in Hz)**	**δ_H mult (*J* in Hz)**	**δ_H mult (*J* in Hz)**	**δ_H mult (*J* in Hz)**	**δ_H mult (*J* in Hz)**	**δ_H mult (*J* in Hz)**
unit	**ring**	**no.**	**major**	**major**	**major A**	**minor B**	**major A**	**minor B**	**rotamer A**	**rotamer B**
I	C	3	4.10, d (3.3)	4.09, d (3.3)	4.09, d (3.3)	3.33, d (3.5)	4.08, d (3.3)	3.28, d (3.5)	4.05, d (3.27)	4.08, d (3.5)
		4	4.45, d (3.3)	4.44, d (3.3)	4.44, d (3.3)	4.22, d (3.5)	4.42, d (3.3)	4.18, d (3.5)	4.39, d (3.31)	4.29, d (3.5)
	A	6	6.04, d (2.4)	6.03, d (2.4)	6.04, d (2.3)	5.98, d (2.3)	6.02, d (2.3)	5.97, d (2.3)	6.00, d (2.34)	6.03, d (2.3)
		8	6.09, d (2.4)	6.08, d (2.4)	6.08, d (2.3)	6.03, d (2.3)	6.07, d (2.3)	6.02, d (2.3)	6.05, d (2.34)	6.07, d (2.3)
	B	2′	7.15, d (2.1)	7.15, d (2.1)	7.15, d (2.1)	7.11, d (2.1)	7.15, d (2.1)	7.11, d (2.1)	7.12, d (2.1)	7.17, d (2.1)
		5′	6.82, d (8.3)	6.81, d (8.3)	6.82, d (8.3)	6.86, d (8.2)	6.82, d (8.2)	6.86, d (8.2)	6.79, d (8.2)	6.84, d (8.2)
		6′	7.03, dd (8.3, 2.1)	7.02, dd (8.3, 2.1)	7.04, dd (8.3, 2.1)	6.90, dd (8.2, 2.1)	7.03, dd (8.2, 2.1)	6.90, dd (8.2, 2.1)	7.00, dd (8.2, 2.1)	7.04, dd (8.2, 2.1)
II	F	2	5.35, s	5.23, s	5.26, s	5.52, s	5.20, s	5.55, s	5.29, s	5.44, s
		3	3.96, brd (2.3)	4.00, brd (2.3)	3.97, brs	4.17, brs	3.92, brd (2.4)	4.18, brd (2.3)	3.89, brd (2.3)	3.84, brd (2.3)
		4	4.74, brs	4.69, brs	4.82, brs	4.53, brs	4.80, brs	4.52, brs	4.55, brs	4.60, brs
	D	6	6.07, s	6.07, s	6.11, s	5.86, s	6.10, s	5.84, s	6.00, s	5.90, s
	E	2′	7.12, d (2.1)	7.12, d (2.1)	7.06, d (2.1)	7.31, d (2.1)	7.05, d (2.1)	7.32, d (2.1)	7.07, d (2.1)	7.03, d (2.1)
		5′	6.78, d (8.2)	6.78, d (8.2)	6.76, d (8.2)	6.83, d (8.2)	6.73, d (8.2)	6.83, d (8.2)	6.75, d (8.2)	6.82, d (8.2)
		6′	6.94, dd (8.2, 2.1)	6.94, dd (8.2, 2.1)	6.91, dd (8.2, 2.1)	7.18, dd (8.2, 2.1)	6.84, dd (8.2, 2.1)	7.19, dd (8.2, 2.1)	6.89, dd (8.2, 2.1)	6.85, dd (8.2, 2.1)
III	I	3	4.12, d (3.6)	4.13, d (3.6)	4.13, d (3.4)	3.68, d (3.2)	4.13, d (3.4)	3.68, d (3.2)	4.19, d (3.4)	4.20, d (3.4)
		4	4.21, d (3.6)	4.33, d (3.6)	4.48, d (3.4)	4.17, d (3.2)	4.48, d (3.4)	4.37, d (3.2)	4.42, d (3.4)	4.31, d (3.4)
	G	6			5.99, s	6.13, s	5.99, s	6.16, s		
		8	6.05, s	6.05, s					6.03, s	6.21, s
	H	2′	7.13, d (2.3)	7.13, d (2.3)	7.30, d (2.2)	7.03, d (2.3)	7.29, d (2.2)	7.02, d (2.2)	7.13, d (2.2)	7.132, d (2.2)
		5′	6.82, d (8.1)	6.82, d (8.1)	6.80, d (8.1)	6.79, d (8.3)	6.79, d (8.1)	6.78, d (8.1)	6.83, d (8.1)	6.81, d (8.1)
		6′	7.02, dd (8.1, 2.3)	7.02, dd (8.1, 2.3)	7.17 dd (8.1, 2.2)	7.01, dd (8.3, 2.3)	7.16, dd (8.1, 2.2)	7.00, dd (8.1, 2.2)	7.03, dd (8.1, 2.2)	7.02, dd (8.1, 2.2)
IV	L	2	4.75, d (8.4)	4.96, brs	4.74, d (8.0)	4.69, d (8.1)	4.93, brs	4.90, brs	5.20, brs	4.94, brs
		3	4.17, m	4.19, m	4.17, m	4.13, m	4.24, m	4.22, m	4.22, m	4.05, m

		4	2.57, dd (−16.2, 9.1)	2.84, brd (−17.0)	2.58, dd (−16.2, 8.5)	2.56, dd (−15.8, 8.8)	2.78a	2.78a	2.88a	2.85a
			3.03, dd (−16.2, 5.4)	2.99, dd (−17.0, 4.6)	2.98, dd (−16.2, 5.4)	2.97, dd (−15.8, 5.5)	2.95a	2.95a	2.91a	2.90a
	J	6	6.12, s	6.14, s	6.04, s	6.16, s	6.04, s	6.15, s	6.10, s	6.11, s
	K	2′	6.99, d (2.1)	7.27, d (2.1)	6.94, d (2.1)	6.93, d (2.1)	7.19, d (2.1)	7.16, d (2.1)	7.09, d (2.1)	7.03, d (2.1)
		5′	6.87, d (8.1)	6.82, d (8.1)	6.84, d (8.1)	6.84, d (8.1)	6.81, d (8.1)	6.82, d (8.1)	6.80, d (8.1)	6.76, d (8.1)
		6′	6.94, dd (8.1, 2.1)	7.00, dd (8.1, 2.1)	6.86, dd (8.1, 2.1)	6.84, dd (8.1, 2.1)	7.02, dd (8.1, 2.1)	6.99, dd (8.1, 2.1)	6.93, dd (8.1, 2.1)	6.59, dd (8.1, 2.1)

[a]Signals are overlapped.

Table 7. ^{13}C NMR Data of 17–22 (CD_3OD, 100 MHz, 278 K)

			17	**18**	**19**		**20**		**21**		**22**
			δ_C	**δ_C**	**δ_C**	**δ_C**	**δ_C**	**δ_C**	**δ_C**	**δ_C**	**δ_C**
unit	**ring**	**no.**	**major**	**major**	**major A**	**minor B**	**major A**	**minor B**	**rotamer A**	**rotamer B**	**major**
I	C	2	100.0	100.1	100.0	99.9	100.1	99.9	100.0	100.0	100.2
		3	68.2	68.3	68.3	67.0	68.3	67.0	68.3	67.8	67.4
		4	29.4	29.4	29.4	28.8	29.4	28.8	29.2	29.1	29.2
	A	5	157.1	157.1	157.1	156.7	157.1	156.8	157.1	156.9	156.5
		6	98.2	98.3	98.1	98.2	98.2	98.2	98.3	98.2	97.8
		7	158.0	158.1	158.0	157.7	158.1	157.8	158.1	158.0	158.1
		8	96.6	96.6	96.5	96.5	96.6	96.5	96.5	96.5	96.5
		9	154.1	154.1	154.1	154.1	154.1	154.1	154.1	154.3	154.0
		10	104.3	104.3	104.2	105.0	104.2	105.1	104.3	104.8	104.1
	B	1′	132.5	132.5	132.5	132.4	132.6	132.5	132.6	132.5	132.2
		2′	115.6	115.6	115.7	115.7	115.5	115.8	115.6	115.6	115.7
		3′	145.6	145.6	145.6	145.4	145.6	145.4	145.8	145.6	145.5
		4′	146.7	146.7	146.7	146.5	146.7	146.6	146.7	146.7	146.7
		5′	115.6	115.5	115.7	115.7	115.8	116.0	115.5–116.0	115.5–116.0	115.7
		6′	119.7	119.7	119.7	119.8	119.7	119.8	119.7	119.9	119.9
II	F	2	78.9	78.7	79.0	78.6	79.0	78.7	78.8	79.4	84.6
		3	72.4	72.4	73.0	72.1	73.1	72.1	72.3	73.1	73.3
		4	38.3	38.5	38.1	38.8	38.2	38.9	38.2	37.3	38.8
	D	5	156.5	156.3	156.5	156.5	156.6	156.7	156.6	156.1	155.5
		6	96.3	96.1	96.4	96.0	96.4	96.0	95.9	96.0	97.5

		7	152.1	152.2	152.4	151.2	152.4	151.2	152.2	151.7	151.3
		8	106.7	106.9	106.9	106.0	107.0	105.9	106.7	106.3	106.7
		9	152.3	152.4	152.4	151.4	152.2	151.4	152.4	152.3	153.0
		10	106.0	105.5	105.5	106.0	105.5	106.1	105.9	106.3	109.3
	E	1′	131.6	131.5	131.5	131.6	131.5	131.7	131.6	131.9	131.1
		2′	116.2	116.2	116.1	116.5	116.1	116.6	116.2	116.0	116.3
		3′	145.8	145.9	145.7	145.9	146.0	145.9	146.0	145.7	146.1
		4′	146.1	146.2	146.1	146.3	146.3	146.3	146.2	146.0	146.2
		5′	115.9	115.9	116.0	116.0	116.0	116.0	115.5–116.0	115.5–116.0	116.0
		6′	120.6	120.7	120.6	121.2	120.6	121.2	120.6	120.3	121.2
III	I	2	100.2	100.1	100.6	99.4	100.6	99.3	100.2	100.3	100.3
		3	67.7	67.7	67.5	67.6	67.8	68.0	67.8	67.8	67.7
		4	29.7	29.6	29.4	29.5	29.5	29.6	29.7	29.3	29.2
	G	5	154.1	154.5	155.2	155.0	155.5	155.1	154.4	154.3	154.0
		6	111.2	110.6	99.1	97.9	99.4	98.2	110.8	111.7	111.6
		7	156.7	156.9	156.8	156.1	156.8	156.2	156.8	156.2	156.8
		8	97.5	97.5	108.6	109.5	108.7	109.8	97.6	96.6	96.0
		9	152.1	152.2	151.2	152.5	152.4	152.7	152.0	152.3	152.0
		10	104.2	104.3	103.7	103.3	104.1	103.8	103.9	104.6	104.4
	H	1′	132.0	132.1	132.2	133.1	132.3	133.3	132.0	132.2	132.5
		2′	115.6	115.6	115.5	115.6	115.5	116.0	115.6	115.6	115.6
		3′	145.6	145.6	145.6	145.7	145.4	145.7	145.7	145.6	145.8
		4′	146.7	146.8	146.7	146.1	146.8	146.3	146.8	146.8	146.8
		5′	115.5	115.6	115.5	115.2	115.6	115.2	115.5–116.0	115.5–116.0	115.5
		6′	119.8	119.8	120.0	120.5	120.0	120.5	119.8	119.9	119.8
IV	L	2	85.1	82.7	84.5	84.5	81.8	81.7	80.9	81.1	80.9
		3	68.2	66.9	68.1	68.2	66.8	67.0	67.2	67.3	67.5
		4	29.2	30.5	29.1	29.2	30.0	30.0	29.5	29.4	29.5
	J	5	156.2	157.0	156.1	155.8	156.7	156.4	156.7	156.7	156.8
		6	96.6	96.7	96.4	96.5	96.5	96.5	96.5	96.8	96.5
		7	152.1	152.2	152.2	152.9	152.2	153.0	152.2	151.9	152.0
		8	106.4	106.8	106.8	107.4	107.2	107.8	106.7	106.9	106.7
		9	151.3	152.2	151.3	150.7	152.4	151.5	151.0	151.1	151.0

		10	103.1	102.2	103.1	102.5	102.3	101.7	101.7	101.7	101.9
	K	1′	130.0	130.5	130.4	130.4	131.3	131.1	131.3	131.5	131.8
		2′	116.3	116.6	115.7	115.7	116.0	115.8	115.0	114.9	114.8
		3′	146.1	145.9	146.2	146.2	146.1	146.0	146.2	146.0	146.2
		4′	146.9	146.7	146.7	146.7	146.0	146.3	146.3	145.4	145.3
		5′	116.8	116.1	116.0	116.0	115.8	115.8	115.5–116.0	116.6	116.8
		6′	121.3	121.4	120.8	120.7	120.4	120.2	119.4	119.3	119.5

Table 8. Comparison of the ^{13}C NMR Resonances of the Terminal Catechol Units in 12, 18, and 20–22 with Those of the Corresponding Carbons in 4 and 6a

	6	**4**	**12**	**12 vs 6**	**12 vs 4**	**18**	**18 vs 6**	**18 vs 4**	**20**	**20 vs 6**	**20 vs 4**	**21**	**21 vs 6**	**21 vs 4**	**22**	**22 vs 6**	**22 vs 4**
no.	**δ_C**	**δ_C**	**δ_C**	**$\Delta\delta_C$**	**$\Delta\delta_C$**	**δ_C**	**$\Delta\delta_C$**	**$\Delta\delta_C$**	**δ_C**	**$\Delta\delta_C$**	**$\Delta\delta_C$**	**δ_C**	**$\Delta\delta_C$**	**$\Delta\delta_C$**	**δ_C**	**$\Delta\delta_C$**	**$\Delta\delta_C$**
2	80.74	81.60	80.79	0.05	–0.81	82.72	1.98	1.12	81.71	0.97	0.11	81.00	0.26	–0.60	80.91	0.17	–0.69
3	67.10	66.93	67.16	0.06	0.23	66.90	–0.20	–0.03	66.94	–0.16	0.01	67.25	0.15	0.31	67.54	0.44	0.61
4	29.51	29.87	29.58	0.07	–0.29	30.50	0.99	0.63	30.00	0.49	0.13	29.43	–0.09	–0.45	29.48	–0.03	–0.39
5	156.65	156.55	156.73	0.08	0.18	156.96	0.31	0.41	156.56	–0.09	0.00	156.73	0.08	0.18	156.80	0.15	0.25
6	96.30	96.31	96.31	0.01	0	96.70	0.40	0.39	96.47	0.17	0.16	96.63	0.33	0.31	96.53	0.23	0.22
7	152.05	152.24	152.05	0	–0.19	152.24	0.19	0.00	152.61	0.55	0.36	152.06	0.00	–0.19	151.97	–0.08	–0.27
8	106.84	107.10	106.96	0.12	–0.14	106.75	–0.09	–0.35	107.51	0.67	0.41	106.80	–0.05	–0.31	106.70	–0.14	–0.40
9	151.28	152.13	151.34	0.06	–0.79	152.40	1.12	0.27	151.94	0.66	–0.19	151.06	–0.22	–1.07	150.95	–0.33	–1.18
10	101.78	102.28	101.88	0.1	–0.4	102.19	0.41	–0.09	102.01	0.22	–0.28	101.71	–0.07	–0.57	101.87	0.09	–0.41
1′	131.37	131.18	131.37	0	0.19	130.47	–0.90	–0.71	131.21	–0.16	0.03	131.39	0.02	0.21	131.76	0.39	0.58
2′	115.07	115.92	115.08	0.01	–0.84	116.60	1.53	0.68	115.90	0.83	–0.02	114.97	–0.10	–0.95	114.80	–0.27	–1.12
3′	146.20	145.88	146.24	0.04	0.36	145.86	–0.34	–0.02	146.05	–0.15	0.17	146.08	–0.12	0.20	146.21	0.01	0.33
4′	146.17	146.17	146.21	0.04	0.04	146.70	0.53	0.53	146.15	–0.02	–0.02	145.84	–0.33	–0.33	145.26	–0.91	–0.91
5′	116.09	115.54	116.11	0.02	0.57	116.07	–0.02	0.53	115.80	–0.29	0.26	NA	NA	NA	116.81	0.72	1.27

6′	119.30	120.29	119.28	–0.02	–1.01	121.41	2.11	1.12	120.33	1.03	0.04	119.36	0.06	–0.93	119.47	0.17	–0.82
$\Sigma\Delta\delta_C$				0.64b	–2.9		8.02	4.48b		4.72	1.18b		–0.08b	–4.17		0.61b	–2.93

[a]^{13}C NMR data (100 MHz) were acquired in CD_3OD with the temperature set as 278 K.

[b]With smaller $\Sigma\Delta\delta_C$ value.

Table 9. Comparison of the ^{13}C NMR Resonances of the Terminal Units in 10 and 15 with Those of the Corresponding Carbons in 2/5 and 4/6a

	2	**5**	**10**	**10 vs 2**	**10 vs 5**	**4**	**6**	**15**	**15 vs 6**	**15 vs 4**
no.	**δ_C**	**δ_C**	**avg δ_C**	**$\Delta\delta_C$**	**$\Delta\delta_C$**	**δ_C**	**δ_C**	**avg δ_C**	**$\Delta\delta_C$**	**$\Delta\delta_C$**
2	84.36	83.75	85.45	1.09	1.70	81.48	80.61	82.66	2.05	1.18
3	68.10	68.29	68.51	0.41	0.22	66.97	67.05	66.92	–0.13	–0.05
4	29.04	28.90	30.17	1.13	1.27	29.90	29.55	30.55	1.00	0.65
5	156.14	156.16	156.30	0.16	0.14	156.56	156.66	156.91	0.25	0.34
6	96.20	96.22	96.56	0.36	0.34	96.12	96.14	96.54	0.40	0.42
7	152.20	152.16	152.2	0.00	0.04	152.24	152.02	152.01	–0.01	–0.23
8	106.60	106.29	106.595	0.00	0.30	107.03	106.75	106.60	–0.15	–0.43
9	151.42	150.79	151.495	0.08	0.71	152.18	151.27	152.40	1.12	0.21
10	102.89	102.58	103.41	0.52	0.83	102.21	101.66	102.19	0.53	–0.02
1′	130.39	130.63	129.74	–0.65	–0.89	131.22	131.33	130.69	–0.64	–0.53
2′	115.56	115.18	116.85	1.29	1.67	115.64	114.91	116.06	1.15	0.42
3′	146.25	146.33	145.67	–0.58	–0.66	145.81	146.16	145.67	–0.49	–0.14
4′	146.70	146.69	146.685	–0.01	0.00	146.08	146.11	146.43	0.32	0.35
5′	116.10	116.14	117.38	1.28	1.24	115.81	115.98	116.56	0.58	0.75
6′	120.64	120.31	120.375	–0.27	0.06	120.18	119.15	121.09	1.94	0.91
$\Sigma\Delta\delta_C$				4.80b	6.97				8.89	4.46b

[a]^{13}C NMR data (100 MHz) were acquired in CD_3OD with the temperature set as 255 K.

[b]With smaller $\Sigma\Delta\delta_C$ value.

Table 10. Comparison of the ^{13}C NMR Resonances of the Terminal Units in 11, 17, and 19 with Those of the Corresponding Carbons in 2 and 5a

	2	5	11	11 vs 2	11 vs 5	17	17 vs 2	17 vs 5	19	19 vs 2	19 vs 5
no	**δ_C**	**δ_C**	**δ_C**	**$\Delta\delta_C$**	**$\Delta\delta_C$**	**δ_C**	**$\Delta\delta_C$**	**$\Delta\delta_C$**	**δ_C**	**$\Delta\delta_C$**	**$\Delta\delta_C$**
2	84.43	83.80	84.44	0.01	0.64	85.1	0.67	1.3	84.49	0.06	0.69
3	68.09	68.32	68.08	–0.01	–0.24	68.18	0.09	–0.14	68.13	0.04	–0.19
4	29.04	28.84	29.18	0.14	0.34	29.22	0.18	0.38	29.14	0.10	0.30
5	156.15	156.14	156.09	–0.06	–0.05	156.15	0	0.01	155.98	–0.17	–0.16
6	96.39	96.37	96.30	–0.09	–0.07	96.60	0.21	0.23	96.45	0.05	0.07
7	152.19	152.17	152.11	–0.08	–0.06	152.08	–0.11	–0.09	152.52	0.33	0.35
8	106.69	106.4	106.79	0.10	0.39	106.39	–0.3	–0.01	107.12	0.43	0.72
9	151.41	150.80	151.36	–0.05	0.56	151.29	–0.12	0.49	151.00	–0.41	0.20
10	103.01	102.69	103.11	0.10	0.42	103.08	0.07	0.39	102.80	–0.22	0.11
1′	130.47	130.77	130.37	–0.10	–0.40	129.95	–0.52	–0.82	130.43	–0.04	–0.34
2′	115.65	115.30	115.83	0.18	0.53	116.31	0.66	1.01	115.70	0.05	0.40
3′	146.30	146.35	146.21	–0.09	–0.14	146.11	–0.19	–0.24	146.20	–0.10	–0.15
4′	146.74	146.70	146.70	–0.04	0.00	146.92	0.18	0.22	146.70	–0.04	0.00
5′	116.22	116.24	116.28	0.06	0.04	116.78	0.56	0.54	116.00	–0.22	–0.24
6′	120.66	120.30	120.81	0.15	0.51	121.31	0.65	1.01	120.74	0.08	0.44
$\Sigma\Delta\delta_C$				0.22b	2.47		2.03b	4.28		–0.06b	2.19

[a]^{13}C NMR data (100 MHz) were acquired in CD_3OD with the temperature set as 278 K.

[b]With smaller $\Sigma\Delta\delta_C$ value.

Results and Discussion

The present study focus on those fractions of the pine bark extract that were enriched in tri- and tetrameric PACs via a two-step centrifugal partition chromatography (CPC) based on dentin bioassay guidance.(9,10) In view of practical limitations posed by bioassay throughput and costs, one valuable means of targeting the isolation of these PACs is to distinguish them from other compounds by following their bright pink-red colored bands on Si gel thin-layer chromatography (TLC) plates after spraying with vanillin–sulfuric acid and heating. A multistep approach for the further purification of enriched bioactive fractions was applied to isolate the 13 PACs. The approach included Sephadex LH-20 and RP-18 column chromatography (CC) with eluents of different selectivity as well as semipreparative HPLC (see the Experimental Section).

The isolation efforts focused on 12.1 g of enriched tri- and tetrameric PACs, obtained upon combining 6.5 g of fraction A and 5.6 g of fraction B that were prepared from 200 g of the pine bark extract by CPC, as described previously.(12) Dentin treated with both fractions A

and B presented statistically higher apparent moduli of elasticity, as compared to control ($p < 0.001$), with an approximate 7- and 9-fold increase in the apparent modulus of elasticity values, respectively. No statistically significant differences occurred among the PAC-treated groups ($p < 0.05$; Figure 2). Considering a certain degree of overlap in constituents as per HPLC and TLC analysis, the materials were combined for the isolation of individual PACs.

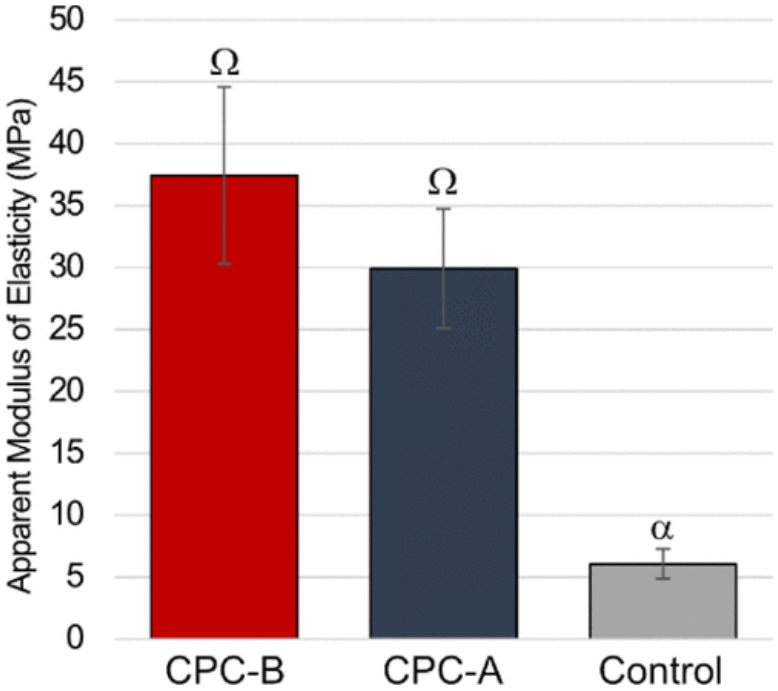

Figure 2. Mean and standard deviation of the apparent modulus of elasticity (MPa) of dentin specimens treated with the CPC fractions A and B. Different symbols depict statistical differences among groups ($p < 0.05$).

Compounds **10** and **17** are the most abundant tri- and tetrameric PACs, respectively, in the investigated pine bark. Their structures are identical with those of the peanut procyanidins D and E,(13) as established by comparison of their ^{1}H and ^{13}C NMR data (Tables 3, 5–7). Phloroglucinolysis of **10** and **17** (Figure 5) further confirmed their structures. Purification of the phloroglucinolysis products resulted in the isolation of **1** and **2** from **10**, as well as **2** and **3** from **17**, respectively. In addition to dimer **2**, the phloroglucinolysis monomer **1** and dimer **3** were used as stereochemical reference points in the subsequent structure elucidation of other trimers and tetramers.

Compound **1** was assigned as 4-phloroglucinol substituted (*ent*)-epicatechin. Its molecular formula $C_{21}H_{18}O_9$ was confirmed based on the (+)-HRESIMS $[M + H]^+$ ion at *m/z* 415.1022 and the ^{13}C NMR carbon counts (Table 1). The relative configuration of **1** was assigned as 2,3-*cis*-

3,4-*trans*, by comparing its ^{13}C NMR resonances of C-2 (δ_C 77.1), C-3 (δ_C 73.2), and C-4 (δ_C 37.0) with the reported values.(14) The observed high-amplitude positive Cotton effect (CE) at 220–240 nm in the ECD spectrum (Figure 3A) of **1** showed that the 4-phloroglucinol group must be β-configured.(15−17) The absolute configuration of **1** was, thus, assigned as (2*R*,3*R*,4*S*)-epicatechin-(4β → 2)-phloroglucinol.

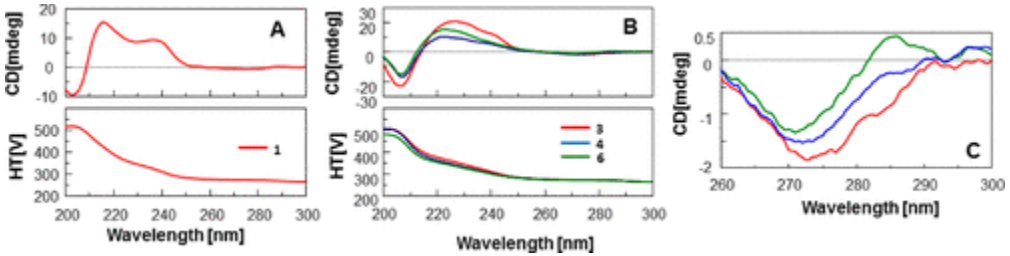

Figure 3. ECD spectra of **1** (A) as well as **3**, **4**, and **6** [(B,C) showing expansions of the 260–300 nm region].

Compound **2** was identified by comparing its ^{1}H and ^{13}C NMR data (Table 2, Figure S6) and ECD (Figure S7) with the reported data.(9) However, based on the analysis of its 2D NMR data, the assignments of several carbon atoms in **2**(9) should be revised as indicated.

Compound **3** was recognized as a phloroglucinol-substituted A-type dimer, and its molecular formula was determined as $C_{36}H_{28}O_{15}$ by the (+)-HRESIMS $[M + H]^+$ ion at *m/z* 701.1504 and the ^{13}C NMR data (Table 1). The ECD spectrum of **3** exhibited a high-amplitude positive CE in the region 220–240 nm (Figure 3B), which assigned the double linkages (2 → O → 7,4 → 8) and the 4-phloroglucinol moiety as being β-oriented. Comparison of the ECD spectra of **3** with those of **4** and **6** revealed that compound **3** exhibited a negative CE in the region 280–290 nm analogous to that of **4** (Figure 3C). The absolute configuration of (2*R*,3*R*) in unit II of **3** was thus determined.(15−17) Considering the diagnostic power of the γ-gauche effect, the upfield shifted C-2 (δ_C 79.1, ring F) when compared to the corresponding carbon in **4** (δ_C 81.5) suggested H-2 and H-4 to be trans-positioned.(18,19) This further corroborated the absolute configuration in unit II as being 2*R*, 3*R*. Accordingly, the structure of **3** had to be epicatechin-(2β → O → 7,4β → 8)-epicatechin-(4β → 2)-phloroglucinol or [PAC **4**]-(4β → 2)-phloroglucinol.

Collectively, this evidence also assigned the structures of the major constituents, **10** and **17**, unambiguously as being assembled by two corresponding moieties, **2** and **4**, assigning them as the trimer, epicatechin-(4β → 6)-[PAC **2**], and the tetramer, [PAC **4**]-(4β → 6)-[PAC **2**].

Compound **9** was purified from the phloroglucinolysis products of **16** and was identified as a phloroglucinol trapped A-type dimer, an assignment supported by its molecular formula $C_{36}H_{28}O_{15}$ as confirmed by the (+)-HRESIMS $[M + H]^+$ peak at *m/z* 701.1546 and the ^{13}C NMR data (Table 1). Analyzing the ^{1}H NMR spectra (Figure S16) of the phloroglucinolysis product of **17** revealed that its products were the same but present in different molar ratios when compared to those of **16**. The products of **17** consisted of **3** as major and **9** as minor in terms of their molar ratio, while **9** was found as major and **3** as minor in phloroglucinolysis products of **16**. Compounds **3** and **9** were, thus, assigned

as C-2 epimerization products during phloroglucinolysis.(20) Accordingly, **9** was recognized as C-2 epimer of **3** and elucidated as [PAC **5**]-(4β → 2)-phloroglucinol.

Compound **11** was isolated and identified in a previous study(9) in which the relative configuration of H-2 and H-4 in the C-ring was determined as being cis-configured based on the NOE between H-2 and H-4 observed in the NOESY spectrum. However, it is known that NOESY data can be ambiguous or inconclusive in the case of spin diffusion. As the previously reported 2,3-*cis*-3,4-*cis* relative configuration of natural PACs is rarely found in the literature, we challenged the prior evidence and pursued additional evidence to establish both the relative and absolute configuration. The upfield shifted C-2 (δ_C 77.1, C-ring; Table 5) when compared to the signal from the corresponding carbon in epicatechin (δ_C 79.1) suggested that H-2 and H-4 are in fact trans-positioned when considering earlier knowledge about the γ-gauche effect.(18,19) Difference in the $J_{3,4}$ values in 2,3-*cis*-3,4-*cis*-(3.8–4.5 Hz) versus 2,3-*cis*-3,4-*trans*-(1–2 Hz) configured moieties further indicated the need to revise the prior assignment of **11** because its $J_{3,4}$ (ca. 1.9 Hz) was congruent with 2,3-*cis*-3,4-*trans* relative configuration.(14,21,22) Reductive cleavage of **11** by phloroglucinol formed compounds **1** and **2**, which were verified by analysis of their MS data and chiral chromatograms (Figure 5). In summary of the new evidence, the structure of **11** should be revised to that of epicatechin-(4β → 8)-[PAC **2**].

Compound **12** shared the molecular formula $C_{45}H_{36}O_{18}$ with **11** based on the (+)-HRESIMS $[M + H]^+$ ion at *m*/*z* 865.1972 and the ^{13}C NMR carbon counts. Comparison of the NMR data (Tables 3 and 5) revealed that **12** is structurally closely related with **11**, with the major differences observed in resonances within unit III. Additionally, close similarities in the ECD curves of **12**, especially the positive CE in the diagnostic 220–240 nm region (Figure 4A), as compared to the ECD of **11**, suggested that the only differences between **12** and **11** were the configurations of C-2 and C-3 in unit III. A cis-configuration of III-H-2 and III-H-3 could be gleaned from the unresolved thus small $J_{2,3}$ value. Accordingly, units II and III had to be linked like in PACs **4** or **6**. Owing to the spatial distance between the upper unit I and the terminal unit III, the chemical shift impact of unit I on unit III had to be small, especially in the ^{13}C domain because of the shielding of the molecular hydrogen "envelope." Differential carbon chemical shift ($\Delta\delta_C$) could, thus, be used to determine the absolute configuration of unit III: units II and III were determined to be doubly connected as in **6** based on the close similarity of the ^{13}C NMR data of the terminal unit III to that of the corresponding carbons in **6** (Table 8). Thereby, the structure of **12** including its absolute configuration was elucidated as epicatechin-(4β → 8)-[PAC **6**]. Although this structure had been reported earlier,(23) the insufficiency of the available NMR data and prior assignment puts its validity into question. Chiral phase HPLC and MS analysis of the phloroglucinolysis products of **12** further confirmed the compound to be assembled from dimer **6** and epicatechin (Figure S104).

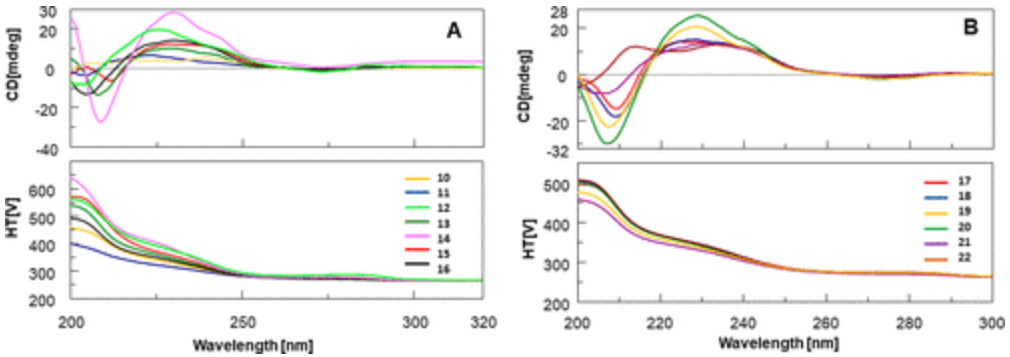

Figure 4. ECD spectra of the trimeric PACs **10–16** (A) and the tetrameric PACs **17–22** (B).

The structure of **13** was established as that of cinnamtannin D1 by comparison of its ^{1}H and ^{13}C NMR data (Tables 3 and 5), as well as its ECD spectrum (Figure 4A) with the reported data.(24−26) Phloroglucinolysis dissociated **13** into two major compounds, **3** and catechin, the structures of which were verified by chiral phase HPLC and MS (Figure S104), collectively confirming **13** as [PAC **4**]-(4β → 8)-catechin, previously named as cinnamtannin D1.

Comparison of their NMR (Tables 3 and 5) and ECD data (Figure 4A) indicated that the structure of **14** was closely related with that of **13**. The major difference was the presence of *para*-hydroxyphenyl signals in **14** versus the AMX ^{1}H NMR resonances of **13**. One pair of highly coupled signals (at δ_H 7.61 and 6.86, each 2H, br d, J = 8.6) was characteristic for a para-substituted phenyl, which was identified as a E-ring via HMBC correlations (Figure S41) connecting II-H-2′&6′ (δ_H 7.61) to II-C-2 (δ_C 78.5). Thus, **14** was shown to contain epiafzelechin as unit II, which was also consistent with the (+)-HRESIMS $[M + H]^+$ peak at *m/z* 849.2045, 16 mass units less than that of **13**. Collectively, the structure of **14** was assigned as II-3′–OH–*nor*-cinnamtannin D1. Phloroglucinolysis with chiral phase HPLC and MS data (Figure S105) affirmed the terminal unit III as catechin.

Compound **15** exhibited a (+)-HRESIMS $[M + H]^+$ peak at *m/z* 865.1960, corresponding to a molecular formula of $C_{45}H_{36}O_{18}$, which was consistent with its ^{13}C NMR data. Compound **15** was thus assigned as a trimeric PAC with one A- and one B-type IFL. Two major rotamers in a ∼3:1 ratio were observed in the ^{1}H and ^{13}C NMR spectra (Tables 4 and 5) acquired at low temperature (255 K) for restricted rotation around the B-type linkage.(9−11,13) The doubly linked interflavanyl bonds (2 → O → 7,4 → 8) between units II and III were verified by the HMBC correlations (Figure S54) from both II-H-4 (δ_H 4.33) and III-H-2 (δ_H 4.95) to III-C-9 (δ_C 152.2). Unit I was attached to unit II through a 4 → 6 bond as derived from the NOESY correlations from II-H-8/II-H-2′ and II-H-6′ (Figure S55), as well as the downfield shifted II-C-6 carbons (avg. δ_C 110.6).(13) The ECD data (Figure 4A) showed a high-amplitude positive CE at 220–240 nm, which assigned a β-configuration to the interflavanyl bonds. Both units I and III were confirmed as (*ent*)-epicatechin based on the singlet signals I-H-2 (δ_H 5.04/5.63, s) and III-H-2 (δ_H 4.95/4.76, s). The upfield shifted chemical shift of the C-ring C-2 carbons (avg δ_C 77.4) suggested H-2 and H-4 to be trans-configured

based on the γ-gauche effect.(18,19) Unit I was, thus, identified as epicatechin with a (2*R*, 3*R*)-absolute configuration. The 3,4-*trans* configuration in the C-ring was assigned based on the NOESY correlation between II-H-3 and III-H-6.(16) Finally, the diagnostic $\Delta\delta_C$ patterns were applied to determine the absolute configuration of the terminal unit III: it was identified as epicatechin as its ^{13}C resonances were significantly closer to those of the corresponding carbons in **4** than to those in **6** (Table 9). To further confirm this conclusion, phloroglucinolysis of **15** was performed. The reaction products were identified as **1** and **4** by MS and chiral phase HPLC (Figure 5). Thus, compound **15** was unambiguously elucidated as epicatechin-(4β → 6)-[PAC **4**]. While this structure has been reported previously,(27) the prior NMR data did not match the present data set. This mismatch can be explained by the incorrect assignment of II-C-10 (δ_C 104.9) in the previous report,(27) which led to establishment of an incorrect 4 → 6 linkage through interpretation of HMBC correlations. The chemical shift previously reported for II-C-6 (δ_C 108.9) better matches the corresponding carbons in **11** and **12**. This indicated that the compound reported earlier(27) in fact had a 4β → 8 IFL. Thus, its structure should be revised to epicatechin-(4β → 8)-epicatechin-(4β → 8,2β → O → 7)-epicatechin.(28) However, considering the subtle substituent chemical shift (s.c.s.) effects uncovered in the present study, it is not surprising that the ^{13}C NMR data corresponding to the structure of epicatechin-(4β → 8)-epicatechin-(4β → 8,2β → O → 7)-epicatechin in refs (27) and (28) are inconsistent. Recognition of such inconsistencies and detection of potential misassignment in PAC structures remain challenging for authors and reviewers alike, and this emphasizes the urgent need for consolidated collections of raw NMR spectroscopic data.(29)

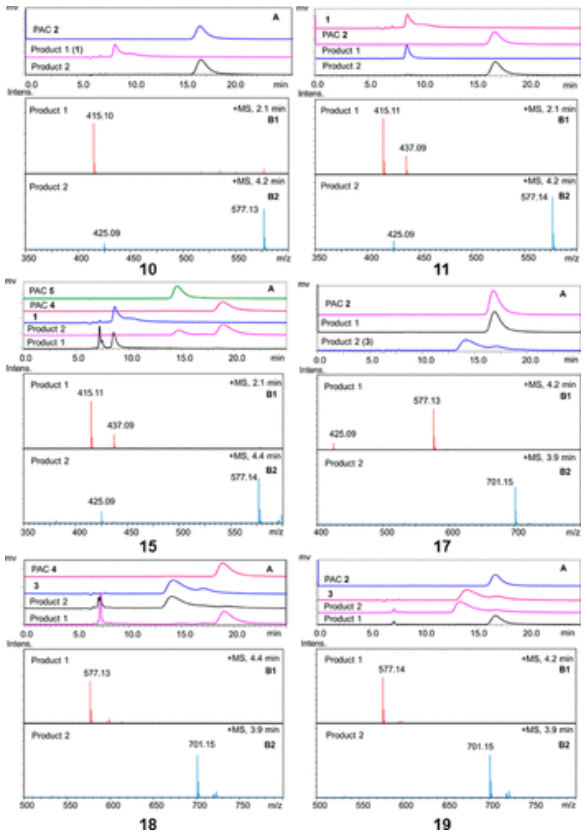

Figure 5. Phloroglucinolysis products of selected **10**, **11**, **15**, and **17–19** identified by chiral phase HPLC and MS analysis.

The A + B-type trimeric PAC nature of **16** was supported by its molecular formula $C_{45}H_{36}O_{18}$, which was established by the (+)-HRESIMS $[M + H]^+$ peak at *m*/*z* 865.2007 and its ^{13}C NMR data. Two sets of ^{1}H NMR data (Table 4) representing two rotamers (~1:1) were observed in the low temperature experiment at 278 K as indicative of the presence of atropisomers in PACs involving B-type IFLs. Both units II and III were identified as (*ent*)-catechin based on the $J_{3,4}$ = 7.6 Hz for unit II and $J_{3,4}$ = (8.4 and 5.4 Hz) for unit III. Units I and II were doubly linked as an A-type dimer through 2 → O → 7/4 → 8 IFLs, as shown by the NOESY cross-peaks from II-H-2′ and II-H-6′ to I-H-4. The terminal unit III was shown to be linked to unit II by a 4 → 6 bond based on the shift of II-C-6 (δ_C 110.8) to lower field when compared to the corresponding carbons II-C-8 (δ_C 108.7) of cinnamtannin D1 and II-C-8 (δ_C 108.8) of aesculitannin B.(25) The β-configuration of both the 2 → O → 7/4 → 8 and the 4 → 6 IFLs were assigned from the positive CE in the diagnostic region 220–240 nm (Figure 4A). Hydrogens II-H-2 and II-H-4 were determined to be cis-positioned based on the similar chemical shifts of II-C-2 (δ_C 84.7) and its corresponding carbon in **5** (δ_C 83.9). This also established the absolute configuration for unit II as 2*S*, 3*R*, and 4*S*. The absolute configuration of I-H-3 was assigned as *R*, based on the

trans-orientation between I-H-3 and I-H-4. This assignment was verified by the NOESY correlation between I-H-3 and II-H-6. Finally, phloroglucinolysis was performed to determine the stereochemistry of the terminal unit III. Analysis of the reaction products revealed the presence of two major compounds: catechin (**8**) and compound **9** (Figure S105), which was found to be [PAC **5**]-(4β → 2)-phloroglucinol. Thus, the structure of **16** was established as [PAC **5**]-(4β → 6)-catechin.

In addition to **17**, five more 2A + B-type tetramers were isolated, as was gleaned from their identical molecular formulas $C_{60}H_{46}O_{24}$ established via HRESIMS (Figures S70, S76, S82, S89, S96, and S103) and associated ^{13}C NMR carbon counts. Comparison of their NMR (Tables 6 and 7) and ECD data (Figure 4B) revealed that **18** had the same planar structure as peanut procyanidin F.(13) Phloroglucinolysis of **18** led to the isolation of two major compounds **3** and **4**, the structures of which were confirmed by MS and chiral phase HPLC (Figure 5). Thus, the structure of **18** was unambiguously determined as [PAC **4**]-(4β → 6)-[PAC **4**].

Analysis of the ^{1}H and ^{13}C NMR spectra of **19**, recorded at 278 K, showed two major rotamers (1.3:1 ratio). Four pairs of resonances for AX spin systems were observed at δ_H 3.33 (d, J = 3.5 Hz), 4.22 (d, J = 3.5 Hz), 3.68 (d, J = 3.2 Hz), and 4.17 (d, J = 3.2 Hz) for rotamer A; and at δ_H 4.09 (d, J = 3.3 Hz), 4.44 (d, J = 3.3 Hz), 4.13 (d, J = 3.2 Hz), and 4.48 (d, J = 3.2 Hz) for rotamer B. This revealed the presence of two doubly linked A-type linkages. Three coupled methines (δ_H 5.52, 4.17, and 4.53 for rotamer A; and δ_H 5.26, 3.92, and 4.82 for rotamer B) indicated the presence of one B-type linkage, which must be located between units II and III as evident from the HMBC correlations (Figure S80) from II-H-4 to III-C-7 and III-C-9. Units II and IV were assigned as (*ent*)-epicatechin and (*ent*)-catechin based on the near 0 Hz value of $J_{2,3}$ in the F-ring and the 8.1 Hz $J_{2,3}$ value in unit IV, respectively. The A-type linkage between units III and IV was confirmed as 2β → O → 7/4β → 8 via the HMBC correlation from IV-H-2 and III-H-4 to IV-C-9, as well as the positive CE at 220–240 nm in the ECD spectrum (Figure 3B). Similarly, the 2β → O → 7/4β → 8 linkage for units I and II was assigned via the NOESY correlations, as shown in Figure S81, between I-H-4 and II-H-2, supported by the ECD data. A 4β → 8 B-type linkage between units II and III was assigned by the NOESY correlations from II-H-4 to III-H-2′, -5′, and -6′, as well as the chemical shifts of III-C-8 in the rotamers (avg. δ_C 109.2 vs 111.2 for **17**). Trans-configuration for H-3 and H-4 was verified by the NOESY correlations from H-3 (C- and I-rings) to H-6 (D- and J-rings, respectively). Trans-positions of H-2 and H-4 in the F-ring was confirmed via the upfield shifted II-C-2 resonances (avg. δ_C 78.8) when compared to the corresponding carbon in **4** (δ_C 81.6). Comparison of the ^{13}C NMR data of unit IV in **19** with the corresponding resonances in **2** and **5** showed that unit IV more closely resembles those in **2** (Table 10). Thus, **19** was confirmed as [PAC **4**]-(4β → 8)-[PAC **2**]. Assignment of MS data and chiral phase HPLC (Figure 5) was consistent with the structures of **3** and **2** as two major phloroglucinolysis products of **19** further confirmed this conclusion.

The ^{1}H and ^{13}C NMR spectra of **20** highly resembled those of **19**, including the presence of two rotamers in a ∼1.5:1 ratio and pointed to the terminal unit IV as the only major difference. The two A- and one B-type linkages in **20** were confirmed in analogy to those in **19** using HMBC (Figure S87), NOESY (Figure S88), ECD (Figure 4B), and ^{13}C NMR data (Table 7). The terminal unit IV was identified as 2,3-*cis*-oriented (*ent*)-epicatechin based on the singlet like δ_H of IV-H-2 in the ^{1}H NMR spectrum. Analysis of the ^{13}C NMR data of unit IV showed that they are much more closely correlated with the corresponding carbons of **4** rather than those of **6** (Table 8). Thus, **19** was established as [PAC **4**]-

(4β → 8)-[PAC **4**], which was further confirmed by phloroglucinolysis (Figure S106). This structure was described previously, and the compound was named as aesculitannin G,(30) although no NMR data were reported.

Based on the similarity of its ^{1}H and ^{13}C NMR data with those of **18**, **21** was recognized as a PAC tetramer in which two A-type dimers were also connected through a B-type IFL. It also showed two major rotamers (∼1:1) in low temperature NMR at 278 K. Both A-type linkages between units I/II and III/IV were confirmed as being 2β → O → 7/4β → 8 via the NOESY correlations (Figure S95) from I-H-4 to II-H-2 and from III-H-4 to IV-H-2′/6′, respectively, as well as through observation of a strong positive CE at 220–240 nm in the ECD spectrum (Figure 4B). A 4β → 6 B-type linkage between units II and III was established by the ECD data and the NOESY correlations from III-H-8 to III-H-2′/6′. The deduction was corroborated by the similar chemical shift of the III-C-6 carbons (avg. δ_C 111.2) relative to those of the corresponding carbons in **17** (avg. δ_C 111.2) and **18** (avg. δ_C 110.9), which were significantly different from those in **19** (avg. δ_C 109.0) and **20** (avg. δ_C 109.2). Unit IV was identified as *ent*-epicatechin based on the closer resemblance of its ^{13}C NMR data to that of **6** relative to those of **4** (Table 8). The structure of **21** was, thus, established as [PAC **4**]-(4β → 6)-[PAC **6**], and this assignment was further confirmed by the identification of **3** and **6** as the phloroglucinolysis products of **21** (Figure S106).

Analysis of the ^{1}H and ^{13}C NMR spectra of **22** revealed that it was also an A + B + A-type tetrameric PAC with two major rotamers (∼2:1 ratio). Units II and IV were assigned as (*ent*)-catechin and (*ent*)-epicatechin, respectively, based on the corresponding $J_{2,3}$ values of 9.6 and ∼0 Hz. A 2β → O → 7/4β → 8 linkage between units I and II was evident from the NOESY correlations (Figure S102) of I-H-4/II-H-2′ and 6′, as well as the high-amplitude CE at 220–240 nm in the ECD spectrum (Figure 4B). Similarly, the 2β → O → 7/4β → 8 A-type linkage between units III and IV was verified by the NOESY correlations of III-H-4/IV-H-2′ and 6′, as well as through ECD evidence. Units II and IV were connected by a 4β → 6 IFL based on the ECD data and the NOESY cross-peaks from III-H-8 to III-H-2′/6′, as well as through the specific chemical shift of III-C-8 (δ_C 111.6). Trans-configuration for H-3 and H-4 in both the C- and I-rings was verified by the NOESY correlations from H-3 (C- and I-ring) to H-6 (D- and J-ring). The *cis*-configuration between H-2 and H-4 in the F-ring was determined via the chemical shift of II-C-2 (δ_C 84.6). Thus, units I and II had to be doubly linked as in **5**. The $\Delta\delta_C$ method was used to determine the absolute configuration of unit IV. Unit IV was identified as *ent*-epicatechin based on the closer resemblance of its ^{13}C NMR resonance patterns with those of corresponding carbons in **6** rather than with those in **4** (Table 8). Collectively, this verified the structure of **22** to be [PAC **5**]-(4β → 6)-[PAC **6**].

Conclusions

The presented combination of chiral spectroscopic (ECD) and chemical (phloroglucinolysis and MS and chiral phase HPLC) analyses generated the necessary framework of chiral reference data that enables the determination of absolute configuration of catechol monomers in oligomeric PACs by one-dimensional (1D) and 2D NMR. Access to the full three-dimensional (3D) structure of PAC trimers, tetramers, and even higher oligomers in their native, underivatized form is critical to establish structure–activity relationships from the subsequent biological evaluation, such as for the dentin biomodification potential of the compounds presented here, which were isolated

from fractions with known bioactivity. The presented structural data expand both our prior reports(9−11) as well as other PAC literatures by providing accurately and precisely assigned ^{13}C NMR resonances. This forms the knowledge base for making absolute stereochemical assignments of PAC monomers via inclusion of the γ-gauche effect observed in the ^{13}C NMR resonances of PACs, as well as the determination of differential ^{13}C chemical shift values (s.c.s; $\Delta\delta_C$) relative to those in the terminal monomers and analogous dimers (here: **2** and **4–6**).

Forming part of a closely knit interdisciplinary approach to PACs as dentin biomodification agents, the present but also previous and ongoing studies have frequently pointed out that the structural complexity of PACs is paired with substantial heterogeneity of the PAC literature in terms of the interplay between reported biological/bioactivity and chemistry/structural information. In this context, robust NMR data play a key role in being most significant for rigor and reproducibility: accurate and precise ^{1}H and ^{13}C assignments and shared spectra are key to achieving consistency among the chemical space of PACs and their biological profiles. While the relatively close resemblance of the spectra of analogous compounds adds to the challenge, the presented outcomes show how unambiguous assignments can transform potentially confusing spectral similarity into definitive structural information. It should be noted that the presence of atropisomeric forms not only dictates the use of low-temperature NMR but also poses a challenge in terms of PAC separation, which can be addressed by applying multiple steps and utilizing a variety of chromatographic techniques with as much as possible orthogonal character (here: countercurrent separation, silica gel-based, and Sephadex LH-20-based size-exclusion/adsorption CC, as well as semipreparative HPLC).

The current study demonstrated the unambiguous elucidation of 13 trimeric and tetrameric PACs by combination of analytical approaches, including HRESIMS, low-temperature NMR, ECD, and phloroglucinolysis with MS and chiral phase HPLC to ensure the correct structure elucidated that use all techniques for each PAC oligomer.

The detailed analysis of ^{13}C NMR data proved to be a key element for achieving absolute stereochemical determination in the monomeric moieties in a series of diastereomeric PACs. Especially, the γ-gauche effect and consideration of s.c.s. effects via comparison of $\Delta\delta_C$ values can corroborate assignments and help detect inconsistencies in the reported data. The presented structures can not only serve as well-characterized components of a small PAC library for the further exploration of their dentin bioactivity but also contribute reliable, fully interpreted, and raw spectroscopic data to the available knowledge base. As high-quality structural data of trimeric and tetrameric PACs is in high demand, the presented outcomes also help avoid future ambiguous or erroneous assignments and increase structural reproducibility and integrity.(29)

Experimental Section

General Experimental Procedures

High-resolution electrospray ionization mass spectrometric measurements were carried out by using a Bruker Impact II, quadrupole time of flight. ECD spectra were acquired on a JASCO-715 spectrometer with a 0.2 cm quartz cuvette, and the sample concentration was less than ≤0.1 mg/mL in MeOH. All 1D/2D NMR spectra were acquired at 255 K, 278 K, and/or 298 K on an 800 MHz Bruker AVANCE spectrometer equipped with a 5 mm triple resonance inverse TCI RT probe. The ^{13}C NMR spectra of all compounds were acquired on a JEOL (Jeol USA, Peabody, MA, USA). A ECZ 400 MHz spectrometer with an FTS cooling system that consists of XR AirJet and TC-84 temperature controller (SP Industries, Warminster, PA, USA). C_{18} reversed-phase (RP-18) silica gel (Macherey-Nagel, Bethlehem, PA, USA) and Sephadex LH-20 gel (Pharmacia, Uppsala, Sweden) were used for CC. TLC was performed on SIL G/UV254 (Macherey-Nagel, Inc., Bethlehem, PA, USA) with visualization under UV light (254 and 365 nm) and spraying with the vanillin–sulfuric acid reagent followed by heating. Semipreparative HPLC was performed on a Shimadzu HPLC (Kyoto, Japan) connected to a PDA detector (Shimadzu, model SPD-20A) and equipped with a YMC-Pack ODS-AQ (250 × 10 mm, S-5, 12 nm) or CHIRAPAK IA (250 × 10.0 mm, *S*-5 μm, Chiral Tech., West Chester, PA, USA). All solvents used were obtained from Fisher Scientific (Fair Lawn, NJ, USA) or Sigma-Aldrich (St. Louis, MO, USA). Phloroglucinol, ascorbic acid, hydrogen chloride, and sodium acetate used were of ACS grade and purchased from Sigma-Aldrich (St. Louis, MO, USA). All NMR solvents were purchased from Cambridge Isotope Laboratories (Tewksbury, MA, USA).

Plant Material

Extract powder of the inner bark of *P. massoniana* was purchased from Xi'an Chukang Biotechnology in China in 2012 (no. PB120212).

Extraction and Isolation

Enriched tri- and tetrameric PACs (12 g), being separated as 6.5 g of fraction A and 5.6 g of fraction B, were prepared from 200 g of the pine bark extract by CPC, as described previously.(12) Both CPC fractions A and B were chromatographed on a Sephadex LH-20 column (EtOH), affording corresponding 6 subfractions (A1–A6) and 7 subfractions (B1–B7), respectively. Fraction A1 (800 mg) contained mainly (±)-catechin and (±)-epicatechin as confirmed by chiral phase HPLC. Fraction A2 (1.0 g) was fractionated over a RP-18 silica gel column (MeOH/H_2O, 20–80%), and the major two subfractions A2b and A2c were then purified to afford compounds **2** (30 mg), **4** (20 mg), **5** (10 mg), and **6** (10 mg) by the semipreparative HPLC (23% MeCN in 0.1% formic acid H_2O, 2.5 mL/min, isocratic). Similarly, after being fractionated by the RP-18 silica gel column, compounds **15** (20 mg); **20** (2.8 mg) and **22** (0.9 mg); as well as **16** (12 mg) and **18** (7.1 mg) were purified from their corresponding fractions A3, A4, and A5, respectively, by semipreparative HPLC (23% MeCN in 0.1% formic acid H_2O, 2.5 mL/min, isocratic). Purification of A6 (1.5 g) via an RP-18 silica gel column (MeOH/H_2O, 25–30%) led to the isolation of the major tetramer, **17** (900 mg). Fraction B5 (800 mg) was fractionated over a RP-18 silica gel column (MeOH/H_2O, 20–80%), and the major three subfractions B5a–B5c were then purified via semipreparative HPLC (18% MeCN in 0.1% formic acid H_2O, 2.5 mL/min) to afford

compounds **11** (30 mg), **12** (1.5 mg), **13** (1.9 mg), and **14** (2.1 mg). Fraction B6 (1.6 g) mainly contained trimer **10** (700 mg), which was purified by a RP-18 silica gel column. Compounds **19** (25 mg) and **21** (2.0 mg) were purified from fraction B7 by semipreparative HPLC (20% MeCN in 0.1% formic acid H_2O, 2.5 mL/min) after prefractionation with an RP-18 silica gel column.

Epicatechin-(4β → 2)-phloroglucinol (1)

Light brown, amorphous solid; ECD (MeOH) λ_{max} (Δε) 203 (−9.6), 216 (+15.4), 237 (+9.3), 275 (−0.7) nm; ^{1}H and ^{13}C NMR (CD_3OD, 255 K), see Table 1, HRMS (ESI) *m*/*z*: $[M + H]^+$ calcd for $C_{21}H_{19}O_9$, 415.1024; found, 415.1022.

Epicatechin-(2β → O → 7,4β → 8)-catechin (2)

Light brown, amorphous solid; ECD (MeOH) λ_{max} (Δε) 208 (−6.8), 222 (+4.2), 272 (−1.4); ^{13}C NMR (CD_3OD, 298, 277, and 255 K), see Table 2; HRMS (ESI) *m*/*z*: $[M + H]^+$ calcd for $C_{30}H_{25}O_{12}$, 577.1341; found, 577.1360.

Epicatechin-(2β → O → 7,4β → 8)-epicatechin-(4β → 2)-phloroglucinol (3)

Light brown, amorphous solid; ECD (MeOH) λ_{max} (Δε) 207 (−23.3), 227 (+20.6), 273 (−1.9); ^{1}H and ^{13}C NMR (CD_3OD, 298 K), see Table 1; HRMS (ESI) *m*/*z*: $[M + H]^+$ calcd for $C_{36}H_{29}O_{15}$, 701.1501; found, 701.1504.

Epicatechin-(2β → O → 7,4β → 8)-epicatechin (4)

Light brown, amorphous solid; ECD (MeOH) λ_{max} (Δε) 207 (−16.9), 222 (+10.4), 272 (−1.5); ^{13}C NMR (CD_3OD, 298, 277, and 255 K), see Table 2; HRMS (ESI) *m*/*z*: $[M + H]^+$ calcd for $C_{30}H_{25}O_{12}$, 577.1341; found, 577.1359.

Epicatechin-(2β → O → 7,4β → 8)-*ent*-catechin (5)

Light brown, amorphous solid; ECD (MeOH) λ_{max} (Δε) 207 (−20.7), 224 (+12.7), 270 (−1.4); ^{13}C NMR (CD_3OD, 298, 277, and 255 K), see Table 2; HRMS (ESI) *m*/*z*: $[M + H]^+$ calcd for $C_{30}H_{25}O_{12}$, 577.1341; found, 577.1357.

Epicatechin-(2β → O → 7,4β → 8)-*ent*-epicatechin (6)

Light brown, amorphous solid; ECD (MeOH) λ_{max} (Δε) 207 (−15.4), 222 (+15.0), 271 (−1.3); ^{13}C NMR (CD_3OD, 298, 277, and 255 K), see Table 2; HRMS (ESI) *m*/*z*: $[M + H]^+$ calcd for $C_{30}H_{24}O_{12}$, 577.1341; found, 577.1348.

Epicatechin-(2β → O → 7,4β → 8)-*ent*-epicatechin-(4β → 2)-phloroglucinol (9)

Light brown, amorphous solid; ^{1}H and ^{13}C NMR (CD_3OD, 298 K), see Table 1; HRMS (ESI) *m*/*z*: $[M + H]^+$ calcd for $C_{36}H_{29}O_{15}$, 701.1501; found, 701.1540.

Epicatechin-(4β → 6)-epicatechin-(2β → O → 7,4β → 8)-catechin (10)

Light brown, amorphous solid; ECD (MeOH) λ_{max} (Δε) 212 (−6.6), 229 (+11); 272 (−1.1); ^{1}H NMR (CD_3OD, 255 K), see Table 3 and ^{13}C NMR (CD_3OD, 255 K), see Table 5, HRMS (ESI) *m/z*: $[M + H]^+$ calcd for $C_{45}H_{37}O_{18}$, 865.1974; found, 865.1996.

Epicatechin-(4β → 8)-epicatechin-(2β → O → 7,4β → 8)-catechin (11)

Light brown, amorphous solid; ECD (MeOH) λ_{max} (Δε) 204 (−4.0), 224 (+6.3), 277 (−0.8); ^{1}H NMR (CD_3OD, 278 K), see Table 3 and ^{13}C NMR (CD_3OD, 278 K), see Table 5. HRMS (ESI) *m/z*: $[M + H]^+$ calcd for $C_{45}H_{37}O_{18}$, 865.1974; found 865.1983.

Epicatechin-(4β → 8)-epicatechin-(2β → O → 7,4β → 8)-*ent*-epicatechin (12)

Light brown, amorphous solid; ECD (MeOH) λ_{max} (Δε) 205 (−8.5), 226 (+19.2), 274 (−2.2), 288 (+1.0); ^{1}H NMR (CD_3OD, 278 K), see Table 3 and ^{13}C NMR (CD_3OD, 278 K), see Table 5, HRMS (ESI) *m/z*: $[M + H]^+$ calcd for $C_{45}H_{37}O_{18}$, 865.1974; found, 865.1972.

Epicatechin-(2β → O → 7,4β → 8)-epicatechin-(4β → 8)-catechin (13)

Light brown, amorphous solid; ECD (MeOH) λ_{max} (Δε) 208 (−13.7), 229 (+9.8), 272 (−1.1); ^{1}H NMR (CD_3OD, 278 K), see Table 3 and ^{13}C NMR (CD_3OD, 278 K), see Table 5, HRMS (ESI) *m/z*: $[M + H]^+$ calcd for $C_{45}H_{37}O_{18}$, 865.1974; found, 865.1966.

Epicatechin-(2β → O → 7,4β → 8)-epiafzelechin-(4β → 8)-catechin (14)

Light brown, amorphous solid; ECD (MeOH) λ_{max} (Δε) 209 (−35.4), 230 (+29.3), 274 (−3.2); ^{1}H NMR (CD_3OD, 278 K), see Table 3 and ^{13}C NMR (CD_3OD, 278 K), see Table 5, HRMS (ESI) *m/z*: $[M + H]^+$ calcd for $C_{45}H_{37}O_{17}$, 849.2025; found, 849.2045.

Epicatechin-(4β → 6)-epicatechin-(2β → O → 7,4β → 8)-epicatechin (15)

Light brown, amorphous solid; ECD (MeOH) λ_{max} (Δε) 212 (−6.6), 229 (+12.0), 272 (−1.1); ^{1}H NMR (CD_3OD, 255 K), see Table 4 and ^{13}C NMR (CD_3OD, 255 K), see Table 5, HRMS (ESI) *m/z*: $[M + H]^+$ calcd for $C_{45}H_{37}O_{18}$, 865.1974; found, 865.1960.

Epicatechin-(2β → O → 7,4β → 8)-*ent*-catechin-(4β → 6)-catechin (16)

Light brown, amorphous solid; ECD (MeOH) λ_{max} (Δε) 204 (−12.8), 229 (+17.2), 274 (−1.3); ^{1}H NMR (CD_3OD, 278 K), see Table 4 and ^{13}C NMR (CD_3OD, 278 K), see Table 5, HRMS (ESI) *m/z*: $[M + H]^+$ calcd for $C_{45}H_{37}O_{18}$, 865.1974; found, 865.1978.

Epicatechin-(2β → O → 7,4β → 8)-epicatechin-(4β → 6)-epicatechin-(2β → O → 7,4β → 8)-catechin (17)

Light brown, amorphous solid; ECD (MeOH) λ_{max} (Δε) 210 (−14.9), 225 (+14.1), 274 (−1.2); ^{1}H NMR (CD_3OD, 278 K), see Table 6 and ^{13}C NMR (CD_3OD, 278 K), see Table 7, HRMS (ESI) *m/z*: $[M + H]^+$ calcd for $C_{60}H_{47}O_{24}$, 1151.2452; found, 1151.2415.

Epicatechin-(2β → O → 7,4β → 8)-epicatechin-(4β → 6)-epicatechin-(2β → O → 7,4β → 8)-epicatechin (18)

Light brown, amorphous solid; ECD (MeOH) λ_{max} (Δε) 209 (−18.2), 229 (+14.8), 273 (−1.1); ^{1}H NMR (CD_3OD, 278 K), see Table 6 and ^{13}C NMR (CD_3OD, 278 K), see Table 7, HRMS (ESI) *m*/*z*: $[M + H]^+$ calcd for $C_{60}H_{47}O_{24}$, 1151.2452; found, 1151.2468.

Epicatechin-(2β → O → 7,4β → 8)-epicatechin-(4β → 8)-epicatechin-(2β → O → 7,4β → 8)-catechin (19)

Light brown, amorphous solid; ECD (MeOH) λ_{max} (Δε) 208 (−22.8), 229 (+20.4), 275 (−1.9); ^{1}H NMR (CD_3OD, 278 K), see Table 6 and ^{13}C NMR (CD_3OD, 278 K), see Table 7, HRMS (ESI) *m*/*z*: $[M + H]^+$ calcd for $C_{60}H_{47}O_{24}$, 1151.2452; found, 1151.2426.

Epicatechin-(2β → O → 7,4β → 8)-epicatechin-(4β → 8)-epicatechin-(2β → O → 7,4β → 8)-epicatechin (20)

Light brown, amorphous solid; ECD (MeOH) λ_{max} (Δε) 208 (−30.1), 229 (+25.2), 274 (−2.3); ^{1}H NMR (CD_3OD, 278 K), see Table 6 and ^{13}C NMR (CD_3OD, 278 K), see Table 7, HRMS (ESI) *m*/*z*: $[M + H]^+$ calcd for $C_{60}H_{47}O_{24}$, 1151.2452; found, 1151.2484.

Epicatechin-(2β → O → 7,4β → 8)-epicatechin-(4β → 6)-epicatechin-(2β → O → 7,4β → 8)-*ent*-epicatechin (21)

Light brown, amorphous solid; ECD (MeOH) λ_{max} (Δε) 206 (−8.2), 232 (+13.1), 273 (−0.8); ^{1}H NMR (CD_3OD, 278 K), see Table 6 and ^{13}C NMR (CD_3OD, 278 K), see Table 7, HRMS (ESI) *m*/*z*: $[M + H]^+$ calcd for $C_{60}H_{47}O_{24}$, 1151.2452; found, 1151.2484.

Epicatechin-(2β → O → 7,4β → 8)-*ent*-catechin-(4β → 6)-epicatechin-(2β → O → 7,4β → 8)-*ent*-epicatechin (22)

Light brown, amorphous solid; ECD (MeOH) λ_{max} (Δε) 214 (+11.8), 225 (+9.7), 236 (+12.8), 273 (−1.5); ^{1}H NMR (CD_3OD, 278 K), see Table 4 and ^{13}C NMR (CD_3OD, 278 K), see Table 7, HRMS (ESI) *m*/*z*: $[M + H]^+$ calcd for $C_{60}H_{47}O_{24}$, 1151.2452; found, 1151.2427.

Phloroglucinolysis

To further confirm the configurations of all the isolated compounds, phloroglucinolysis was performed.(20) Compounds **10** (10 mg) and **17** (10 mg) were individually cleaved using a reaction mixture consisting of 400 mg of phloroglucinol and 100 mg of ascorbic acid in 10 mL of 0.1 N HCl in MeOH at 50 °C for 30 min. Adding 50 mL of 40 mM sodium acetate solution to the mixture stopped the reaction. The mixture was then extracted twice with ethyl acetate, and the concentrated ethyl acetate layer was loaded onto Sephadex LH-20 for purification and resulted in the isolation of **1** and **2** from **10**, as well as **2** and **3** from **17**. Similarly, phloroglucinolysis of **11** (5.5 mg), **15** (3.1 mg), **16** (2.8 mg), **18** (3.0 mg), and **19** (3.1 mg) by 100 mg of phloroglucinol and 50 mg of ascorbic acid in 5 mL of 0.1 N HCl in MeOH at 50 °C for 30 min was performed. Each reaction mixture was extracted by ethyl acetate, and then purified as corresponding two products as being confirmed by chiral phase HPLC and MS data. About 0.3–0.5 mg of **12–14**, **20**, and **21** were cleaved using a reaction mixture consisting of 20 mg of phloroglucinol and 10 mg of ascorbic acid in 2 mL of 0.1 N HCl in MeOH at 50 °C for 30 min. The identity of all reaction products was confirmed by chiral phase HPLC and MS analysis.

Dental Bioassay

Dentin fragments were sectioned into 0.5 × 1.7 × 7.0 mm (*H* × *W* × *L*) pieces and demineralized using 10% phosphoric acid for 5 h. Specimens were treated with the compounds at 0.65% w/v in 20 mM 4-(2-hydroxyethyl)-1-piperazineethanesulfonic acid (HEPES) buffer (pH 7.2) for 1 h, and a control group was kept in HEPES buffer only (*n* = 5). The apparent modulus of elasticity (*E*) was measured using a 3-point bending method with a universal testing machine, as described previously.(31) Data were statistically evaluated by one-way ANOVA and Tukey's post hoc tests (α = 0.05).

References

1 Ferreira, D.; Bekker, R. Oligomeric proanthocyanidins: naturally occurring O-heterocycles. *Nat. Prod. Rep.* **1996**, *13*, 411– 433, DOI: 10.1039/np9961300411

2 Hümmer, W.; Schreier, P. Analysis of proanthocyanidins. *Mol. Nutr. Food Res.* **2008**, *52*, 1381– 1398, DOI: 10.1002/mnfr.200700463

3 Schwitters, B. *OPC in Practice: The Hidden Story of Proanthocyanidins, Nature's Most Powerful and Patented Antioxidant*; Alfa Omega Editrice, 1995.

4 Škerget, M.; Kotnik, P.; Hadolin, M.; Hraš, A. R.; Simonič, M.; Knez, Ž. Phenols, proanthocyanidins, flavones and flavonols in some plant materials and their antioxidant activities. *Food Chem.* **2005**, *89*, 191– 198, DOI: 10.1016/j.foodchem.2004.02.025

5 Kim, Y.-J. Anticancer effects of oligomeric proanthocyanidins on human colorectal cancer cell line, SNU-C4. *World J. Gastroenterol.* **2005**, *11*, 4674– 4678, DOI: 10.3748/wjg.v11.i30.4674

6 Li, W. G.; Zhang, X. Y.; Wu, Y. J.; Tian, X. Anti-inflammatory effect and mechanism of proanthocyanidins from grape seeds. *Acta Pharmacol. Sin.* **2001**, *22*, 1117– 1120

7 Anderson, R. A.; Broadhurst, C. L.; Polansky, M. M.; Schmidt, W. F.; Khan, A.; Flanagan, V. P.; Schoene, N. W.; Graves, D. J. Isolation and characterization of polyphenol type-A polymers from cinnamon with insulin-like biological activity. *J. Agric. Food Chem.* **2004**, *52*, 65– 70, DOI: 10.1021/jf034916b

8 Mandel, S.; Youdim, M. B. H. Catechin polyphenols: neurodegeneration and neuroprotection in neurodegenerative diseases. *Free Radical Biol. Med.* **2004**, *37*, 304– 317, DOI: 10.1016/j.freeradbiomed.2004.04.012

9 Nam, J.-W.; Phansalkar, R. S.; Lankin, D. C.; Bisson, J.; McAlpine, J. B.; Leme, A. A.; Vidal, C. M. P.; Ramirez, B.; Niemitz, M.; Bedran-Russo, A.; Chen, S.-N.; Pauli, G. F. Subtle chemical shifts explain the NMR fingerprints of oligomeric proanthocyanidins with high dentin biomodification potency. *J. Org. Chem.* **2015**, *80*, 7495– 7507, DOI: 10.1021/acs.joc.5b01082

10 Nam, J.-W.; Phansalkar, R. S.; Lankin, D. C.; McAlpine, J. B.; Leme-Kraus, A. A.; Vidal, C. M. P.; Gan, L.-S.; Bedran-Russo, A.; Chen, S.-N.; Pauli, G. F. Absolute configuration of native oligomeric proanthocyanidins with dentin biomodification potency. *J. Org. Chem.* **2017**, *82*, 1316– 1329, DOI: 10.1021/acs.joc.6b02161

11 Phansalkar, R. S.; Nam, J.-W.; Leme-Kraus, A. A.; Gan, L.-S.; Zhou, B.; McAlpine, J. B.; Chen, S.-N.; Bedran-Russo, A. K.; Pauli, G. F. Proanthocyanidin dimers and trimers from *Vitis vinifera* provide diverse structural motifs for the evaluation of dentin biomodification. *J. Nat. Prod.* **2019**, *82*, 2387– 2399, DOI: 10.1021/acs.jnatprod.8b00953

12 Phansalkar, R. S.; Nam, J.-W.; Chen, S.-N.; McAlpine, J. B.; Leme, A. A.; Aydin, B.; Bedran-Russo, A.-K.; Pauli, G. F. Centrifugal partition chromatography enables selective enrichment of trimeric and tetrameric proanthocyanidins for biomaterial development. *J. Chromatogr. A* **2018**, *1535*, 55– 62, DOI: 10.1016/j.chroma.2017.12.050

13 Dudek, M. K.; Gliński, V. B.; Davey, M. H.; Sliva, D.; Kaźmierski, S.; Gliński, J. A. Trimeric and tetrameric A-type procyanidins from peanut skins. *J. Nat. Prod.* **2017**, *80*, 415– 426, DOI: 10.1021/acs.jnatprod.6b00946

14 Foo, L. Y.; Karchesy, J. J. Procyanidin polymers of *Douglas fir* bark: Structure from degradation with phloroglucinol. *Phytochemistry* **1989**, *28*, 3185– 3190, DOI: 10.1016/0031-9422(89)80303-6

15 Slade, D.; Ferreira, D.; Marais, J. P. J. Circular dichroism, a powerful tool for the assessment of absolute configuration of flavonoids. *Phytochemistry* **2005**, *66*, 2177– 2215, DOI: 10.1016/j.phytochem.2005.02.002

16 Kolodziej, H.; Sakar, M. K.; Burger, J. F. W.; Engelshowe, R.; Ferreira, D. A-type proanthocyanidins from *Prunus spinosa*. *Phytochemistry* **1991**, *30*, 2041– 2047, DOI: 10.1016/0031-9422(91)85064-7

17 Botha, J. J.; Young, D. A.; Ferreira, D.; Roux, D. G. Synthesis of condensed tannins. Part 1. Stereoselective and stereospecific syntheses of optically pure 4-arylflavan-3-ols, and assessment of their absolute stereochemistry at C-4 by means of circular dichroism. *J. Chem. Soc., Perkin Trans. 1* **1981**, 1213– 1219, DOI: 10.1039/p19810001213

18 Lokman Khan, M.; Haslam, E.; Williamson, M. P. Structure and conformation of the procyanidin B-2 dimer. *Magn. Reson. Chem.* **1997**, *35*, 854– 858, DOI: 10.1002/(sici)1097-458x(199712)35:12<854::aid-omr184>3.0.co;2-n

19 Cai, Y.; Evans, F. J.; Roberts, M. F.; Phillipson, J. D.; Zenk, M. H.; Gleba, Y. Y. Polyphenolic compounds from *Croton lechleri*. *Phytochemistry* **1991**, *30*, 2033– 2040, DOI: 10.1016/0031-9422(91)85063-6

20 Kennedy, J. A.; Jones, G. P. Analysis of proanthocyanidin cleavage products following acid-catalysis in the presence of excess phloroglucinol. *J. Agric. Food Chem.* **2001**, *49*, 1740– 1746, DOI: 10.1021/jf001030o

21 van der Westhuizen, J. H.; Ferreira, D.; Roux, D. G. Synthesis of condensed tannins. Part 2. Synthesis by photolytic rearrangement, stereochemistry, and circular dichroism of the first 2,3-cis-3,4-cis-4-arylflavan-3-ols. *J. Chem. Soc., Perkin Trans. 1* **1981**, 1220– 1226, DOI: 10.1039/p19810001220

22 Kozikowski, A. P.; Tückmantel, W.; Hu, Y. Studies in Polyphenol Chemistry and Bioactivity. Stereocontrolled Synthesis of Epicatechin-4α,8-epicatechin, an Unnatural Isomer of the B-Type Procyanidins. *J. Org. Chem.* **2001**, *66*, 1287– 1296, DOI: 10.1021/jo001462y

23 Wang, Y.; Singh, A. P.; Hurst, W. J.; Glinski, J. A.; Koo, H.; Vorsa, N. Influence of degree-of-polymerization and linkage on the quantification of proanthocyanidins using 4-dimethylaminocinnamaldehyde (DMAC) assay. *J. Agric. Food Chem.* **2016**, *64*, 2190– 2199, DOI: 10.1021/acs.jafc.5b05408

24 Lin, H.-C.; Lee, S.-S. Proanthocyanidins from the Leaves of *Machilus philippinensis*. *J. Nat. Prod.* **2010**, *73*, 1375– 1380, DOI: 10.1021/np1002274

25 Dudek, M. K.; Kazmierski, S.; Stefaniak, K.; Glinski, V. B.; Glinski, J. A. Conformational equilibria in selected A-type trimeric procyanidins. *Org. Biomol. Chem.* **2014**, *12*, 9837– 9844, DOI: 10.1039/c4ob02086c

26 Satake, T.; Kamiya, K.; Ohno, A.; Horii, Y.; Endang, H.; Umar, M. A-type proanthocyanidins from the bark of *Parameria laevigata*. *Heterocycles* **2003**, *60*, 1697– 1708, DOI: 10.3987/com-03-9793

27 Foo, L. Y.; Lu, Y.; Howell, A. B.; Vorsa, N. A-Type Proanthocyanidin Trimers from Cranberry that Inhibit Adherence of Uropathogenic P-Fimbriated *Escherichia coli*. *J. Nat. Prod.* **2000**, *63*, 1225– 1228, DOI: 10.1021/np000128u

28 Xu, X.; Xie, H.; Wang, Y.; Wei, X. A-Type proanthocyanidins from lychee seeds and their antioxidant and antiviral activities. *J. Agric. Food Chem.* **2010**, *58*, 11667– 11672, DOI: 10.1021/jf1033202

29 McAlpine, J. B.; Chen, S.-N.; Kutateladze, A.; MacMillan, J. B.; Appendino, G.; Barison, A.; Beniddir, M. A.; Biavatti, M. W.; Bluml, S.; Boufridi, A.; Butler, M. S.; Capon, R. J.; Choi, Y. H.; Coppage, D.; Crews, P.; Crimmins, M. T.; Csete, M.; Dewapriya, P.; Egan, J. M.; Garson, M. J.; Genta-Jouve, G.; Gerwick, W. H.; Gross, H.; Harper, M. K.; Hermanto, P.; Hook, J. M.; Hunter, L.; Jeannerat, D.; Ji, N.-Y.; Johnson, T. A.; Kingston, D. G. I.; Koshino, H.; Lee, H.-W.; Lewin, G.; Li, J.; Linington, R. G.; Liu, M.; McPhail, K. L.; Molinski, T. F.; Moore, B. S.; Nam, J.-W.; Neupane, R. P.; Niemitz, M.; Nuzillard, J.-M.; Oberlies, N. H.; Ocampos, F. M. M.; Pan, G.; Quinn, R. J.; Reddy, D. S.; Renault, J.-H.; Rivera-Chávez, J.; Robien, W.; Saunders, C. M.; Schmidt, T. J.; Seger, C.; Shen, B.; Steinbeck, C.; Stuppner, H.; Sturm, S.; Taglialatela-Scafati, O.; Tantillo, D. J.; Verpoorte, R.; Wang, B.-G.; Williams, C. M.; Williams, P. G.; Wist, J.; Yue, J.-M.; Zhang, C.; Xu, Z.; Simmler, C.; Lankin, D. C.; Bisson, J.; Pauli, G. F. The value of universally available raw NMR data for transparency, reproducibility, and integrity in natural product research. *Nat. Prod. Rep.* **2019**, *36*, 35– 107, DOI: 10.1039/c7np00064b

30 Morimoto, S.; Nonaka, G.-I.; Nishioka, I. Tannins and related compounds. LIX. Aesculitannins, novel proanthocyandins with doubly-bonded structures from *Aesculus hippocastanum* L. *Chem. Pharm. Bull.* **1987**, *35*, 4717– 4729, DOI: 10.1248/cpb.35.4717

31 Vidal, C. M. P.; Aguiar, T. R.; Phansalkar, R.; McAlpine, J. B.; Napolitano, J. G.; Chen, S.-N.; Araújo, L. S. N.; Pauli, G. F.; Bedran-Russo, A. Galloyl moieties enhance the dentin biomodification potential of plant-derived catechins. *Acta Biomater.* **2014**, *10*, 3288– 3294, DOI: 10.1016/j.actbio.2014.03.036

32 Zhou, B.; Alania, Y.; Reis, M.; Phansalkar, R.; Nam, J.-W.; McAlpine, J.; Chen, S.-N.; Bedran-Russo, A.; Pauli, G. F. Tri- and Tetrameric Proanthocyanidins with Dentin Bioactivities from *Pinus massoniana*. **2020**, chemrxiv:12055389.